Unveiling the role of spatial transcriptomics in the analysis of the tumor immune microenvironment (Review)

JIALIN JIANG[1-3*], XINYU TU[1-3*], YI CAO[1-3*], QUN YAN[4], BUQING SAI[5] and JIAN MA[1-3]

[1]Hunan Key Laboratory of Cancer Metabolism, Hunan Cancer Hospital/The Affiliated Cancer Hospital of Xiangya School of Medicine, Central South University, Changsha, Hunan 410013, P.R. China; [2]Cancer Research Institute, Xiangya School of Basic Medicine Sciences, Central South University, Changsha, Hunan 410078, P.R. China; [3]Key Laboratory of Carcinogenesis and Cancer Invasion of The Chinese Ministry of Education, NHC Key Laboratory of Carcinogenesis, Hunan Key Laboratory of Nonresolving Inflammation and Cancer, Changsha, Hunan 410078, P.R. China; [4]Department of Clinical Laboratory, Xiangya Hospital, Central South University, Changsha, Hunan 410008, P.R. China; [5]Department of Biochemistry and Molecular Biology, School of Basic Medicine, Kunming Medical University, Kunming, Yunnan 650500, P.R. China

Received March 3, 2026; Accepted June 23, 2026

DOI: 10.3892/ijmm.2026.5940

Abstract. The tumor immune microenvironment plays a decisive role in tumor initiation, progression and therapeutic response. Spatial transcriptomics (ST) enables comprehensive analysis of the whole transcriptome or specific gene sets while preserving the original spatial location information within tissues, offering a revolutionary approach to unraveling the complexity of the tumor immune microenvironment in the spatial dimension. The present review aims to systematically elaborate on the role and application of ST in deciphering the tumor immune microenvironment. Focusing on tumor microenvironment niches at different stages of tumor progression, from precancerous lesions and locally advanced tumors to distant metastasis, recent advances in ST for mapping the spatial distribution and functional states of key cell subpopulations are summarized. The present review further highlights its potential for clinical translation in identifying spatially defined biomarkers and elucidating the mechanisms underlying therapeutic responses and analyze the key technical challenges that constrain the application of ST in clinical practice. In recent years, the rapid development of machine learning algorithms has provided new opportunities to overcome the technical limitations of ST. The deep integration of machine learning with ST is laying a solid theoretical foundation and technical support for precision medicine and early intervention.

Contents

1. Introduction

The tumor immune microenvironment is a key factor determining tumor initiation, progression and therapeutic response (1,2). Its spatial heterogeneity and complex intercellular interactions have long been challenging to decipher. Although traditional single-cell sequencing technologies can reveal cellular diversity, they lose vital spatial location information. The emergence of spatial transcriptomics (ST) has provided a revolutionary tool for analyzing the tumor immune microenvironment in spatial dimensions by preserving *in situ* spatial coordinates while detecting whole-transcriptome or specific gene set expression (3,4).

ST technologies have been widely applied across diverse cancer types, systematically revealing the spatial organization and functional states of different cell populations within the tumor immune microenvironment. These technologies enable the precise localization of key cell subsets and the effective identification of tumor niches with key biological functions,

Correspondence to: Dr Buqing Sai, Department of Biochemistry and Molecular Biology, School of Basic Medicine, Kunming Medical University, 1168 Chunrongxi Road, Chenggong, Kunming, Yunnan 650500, P.R. China
E-mail: saibuqing@kmmu.edu.cn

Dr Jian Ma, Hunan Key Laboratory of Cancer Metabolism, Hunan Cancer Hospital/The Affiliated Cancer Hospital of Xiangya School of Medicine, Central South University, 283 Tongzipo Road, Yuelu, Changsha, Hunan 410013, P.R. China
E-mail: majian@csu.edu.cn

*Contributed equally

Key words: spatial transcriptomics, tumor immune microenvironment, machine learning, multi-omics analysis, personalized therapy

including tertiary lymphoid structures (TLS), immune exclusion niches and tumor invasion front niches (5,6). The present review systematically summarizes the core advances of ST in elucidating the composition of the tumor microenvironment (TME), the spatiotemporal logic of immune escape and the evaluation of clinical significance across distinct stages of tumor progression, from premalignant lesions and locally advanced disease to distant metastasis.

The fine-resolution molecular information provided by ST is driving disease subtyping, prognostic prediction and treatment response assessment toward greater precision, a progress particularly pronounced in oncology. Studies (7-10) have shown that the spatial molecular landscape of tumors is closely associated with their growth behavior, metastatic potential, and response to immunotherapy, highlighting the value of this technology in two clinically translational directions: The discovery of spatial context-associated biomarkers and the elucidation of molecular mechanisms underlying therapeutic response. However, the practical application of ST in clinical diagnosis and decision-making still faces a series of key challenges, including insufficient resolution, limited sample representativeness, risk of algorithmic bias and lack of cross-platform standardization. The rapid advancement of machine learning has provided new opportunities to address these technical bottlenecks (11). As multi-omics technologies and machine learning become increasingly integrated, with continued breakthroughs in multimodal data integration and three-dimensional tissue reconstruction, the understanding of tumor evolution will continue to deepen.

2. Overview of spatial transcriptomics

The emergence of spatial transcriptomics. Single-cell RNA sequencing (scRNA-seq) technologies have evolved from initial transcriptome profiling to encompass multiple omics dimensions, including three-dimensional genomics, epigenomics and proteomics, and have even enabled high-throughput single-cell multi-omics sequencing (12-16). These advancements have become key drivers across a wide range of research areas (17). ScRNA-seq is used to profile RNA expression in individual cells, providing insights into cell-type-specific functions under specific conditions. However, scRNA-seq requires dissociating cells from their native tissue microenvironment. During this dissociation process, cells lose their original spatial context, thereby precluding the detection of influences from neighboring cells or the surrounding environment, as well as the coordinated relationship between spatial organization and cellular function. ST integrates molecular biology with histology techniques, enabling direct mapping of RNA molecule distributions on tissue sections and resolving the spatial features of gene expression. This approach thus overcomes a fundamental limitation of scRNA-seq (18). Based on their underlying molecular detection principles, ST technologies can be broadly classified into two main categories: Sequencing-based and imaging-based ST technologies.

Technical classifications and platform comparisons

Sequencing-based ST technologies. Sequencing-based ST technologies originated from single-cell sequencing. In 2016, Stahl *et al* (19) first proposed a ST method based on spatial barcoding, which has since been widely adopted. This technique enables whole-transcriptome capture by converting the cell barcodes used in single-cell sequencing into spatial location barcodes and replacing bead-based single-cell capture with fixed-size, spatially defined spots on a chip. It then employs amplification and sample indexing principles similar to those of single-cell transcriptome sequencing to achieve high-throughput spatial transcriptome sequencing. Several improved, novel sequencing-based ST technologies have emerged, including 10x Genomics Visium (20), Slide-Seq (21) and Stereo-seq (22). Visium offers enhanced resolution and sensitivity, is widely used in neuroscience, cancer research, and developmental biology, and benefits from a mature commercial platform and standardized experimental protocols, including support for formalin-fixed and paraffin-embedded (FFPE) samples. Slide-Seq uses randomly deposited barcoded beads on a slide for mRNA capture, providing higher resolution suitable for applications such as nervous system mapping or liver lobule zonation; however, the stochastic distribution of beads may affect data consistency. Stereo-seq achieves nanoscale resolution, enabling subcellular-level analysis, which makes it suitable for tissue mapping in contexts such as embryonic development, although its demanding experimental requirements pose certain limitations (summarized in Table I).

Notably, differences in sensitivity, throughput, resolution and other parameters across ST platforms directly determine the robustness of the same biological conclusion under different technological settings. Taking resolution and sensitivity as an example, Visium's 55 μm resolution mixes an average of 3-10 cells per spot, smoothing out cellular heterogeneity. As a result, conclusions that depend on rare cell types or low-abundance genes may be lost due to signal dilution. By contrast, Slide-Seq (10 μm) and Stereo-seq (500 nm) achieve single-cell to subcellular resolution. However, when the analytical unit is reduced to the pixel level in Stereo-seq, the robustness of its conclusions becomes highly dependent on the accuracy of subcellular pixel clustering algorithms, different algorithms may lead to radically different definitions of cell boundaries and divergent conclusions regarding gene localization.

More importantly, differences in analytical assumptions fundamentally determine whether the aforementioned hardware metrics can be translated into reliable biological conclusions. Specifically: Visium operates on the assumption that 'gene expression within each 55 μm spot represents the average state of that region'. This assumption holds in tissues with uniformly distributed cell types. However, in highly heterogeneous microenvironments (for example, tumor-immune boundaries), the mixed signal within a spot can lead to a conclusion of 'high gene expression' that is actually a summation artifact of multiple cell types rather than a true feature of any single cell type. Slide-Seq assumes that 'mRNA captured by a single 10 μm bead originates primarily from a single cell'. This assumption approximately holds in tissues with large, loosely packed cells (for example, cerebral cortex). But in cell-dense tissues (for example, embryonic tissues) or samples with abundant cell debris, it is common for a single bead to simultaneously capture mRNA from multiple cells, rendering the 'one bead=one cell' analytical premise invalid and leading to cell type annotation errors. Stereo-seq assumes that 'signals from 500 nm DNA nanoball (DNB) spots can

Table I. Comparison of sequencing-based spatial transcriptomics technologies.

Core performance parameters	10x Genomics visium	Slide-seq	Stereo-seq
Transcript capture strategy	Oligonucleotides containing spatial barcodes and capture sequences are pre-synthesized on defined spots (55 μm in diameter) on a glass slide, with the positional barcode of each spot decoded via sequencing. After tissue section attachment, mRNA diffuses to the capture spots through permeation for binding.	A monolayer of 10 μm beads coated with random barcode DNA oligonucleotides is arrayed on a glass slide. The spatial position of each bead is decoded via SOLiD sequencing, followed by tissue section attachment for mRNA capture.	A patterned array of DNBs serves as the capture substrate, with each DNB carrying a spatial barcode and a poly-T capture sequence. The high-density DNB array generated by rolling circle amplification achieves ultra-high resolution.
Resolution	55 μm	10 μm	500 nm
Detection sensitivity	~500 UMIs per 100 μm^2	~550 UMIs per 100 μm^2 for the V2 version.	~1,450 UMIs per 100 μm^2
Throughput and capture area	Moderate. One slide contains four capture areas (6.5x6.5 mm^2 each), allowing 1-4 samples to be processed simultaneously. Gene read throughput depends on sequencing depth.	Low to moderate. A single slide typically accommodates only one sample (6.2x6.2 mm^2), resulting in low sample throughput. However, the gene detection throughput at the single-cell/per-spot level is very high.	High. A single chip can accommodate multiple samples (up to 13.2 cmx13.2 cm). The large capture area combined with high resolution yields exceptionally high data output.
Tissue compatibility	FFPE (strong)/FF	FF (main)	FF (main)
Primary applications	Large-scale tissue gene expression analysis, suitable for liver, tumor, neural tissues.	Studies of nervous system, liver lobule zonation.	Ultra-high-resolution tissue mapping, for example, embryonic development, tumors
Advantages	Mature commercial platform, standardized workflow, supports FFPE samples	Higher resolution than 10x Visium, supports whole transcriptome sequencing	Extremely high resolution, allows subcellular analysis, suitable for large tissues
Limitations	Low resolution, insufficient for single-cell level analysis	Limited capture area, random bead distribution affects data consistency	High computational demand, stringent experimental requirements

FFPE, formalin-fixed paraffin-embedded; seq, sequencing; DNB, DNA nanoballs.

be accurately reconstructed into true cell boundaries through post hoc clustering (binning)'. However, this assumption faces fundamental challenges in practice, the choice of clustering bin size (for example, bin50 vs. bin100) lacks a gold standard, and different sizes may yield mutually contradictory subcellular localization conclusions. More importantly, mRNA captured by DNB spots may originate from cellular protrusions (for example, neuronal axons or tumor pseudopodia) located hundreds of nanometers away, in which case the 'clustering reconstructs cell boundaries' assumption is biologically invalid. Therefore, any subcellular localization conclusion requires independent validation (for example, by spatial *in situ* hybridization) to confirm its robustness.

Imaging-based spatial transcriptomics technologies. Imaging-based ST technologies function by designing fluorescently labeled oligonucleotide probes that hybridize *in situ* with target RNAs, directly converting RNA molecular information into localizable and quantifiable fluorescence signals. These primarily include *in situ* sequencing (ISS) and *in situ* hybridization (ISH). Specifically, in ISS, RNA is reverse transcribed, amplified via rolling circle amplification (RCA), and sequenced *in situ*; this method has been applied in research related to cancer, tuberculosis and other diseases (23-26). Classic ISH techniques include multiplexed error-robust fluorescence *in situ* hybridization (MERFISH) (27) and sequential fluorescence ISH (seqFISH) (28), among others. In MERFISH, multiple rounds of hybridization and imaging are performed to detect the presence or absence of fluorescently labeled probes. Subsequently, sequential images are decoded using error-robust barcodes associated with each transcript's identity (27,29,30). MERFISH offers extremely high resolution and has been widely used for gene expression studies at single-cell and subcellular levels. seqFISH (31,32) is similar to MERFISH and is suitable for subcellular-level research, particularly in immunology. Both techniques can detect up to 10,000 target genes with subcellular resolution (28,33).

Table II. Comparison of imaging-based spatial transcriptomics technologies.

Core performance parameters	MERFISH	seqFISH/seqFISH+	ISS
Transcript capture strategy	A combinatorial binary encoding strategy is used. Each mRNA is assigned an N-bit binary barcode, which is read out through the presence or absence (1/0) of fluorescent probes across multiple imaging rounds. Error-correcting codes (for example, Hamming distance) are employed to ensure detection accuracy.	Through multiple rounds of hybridization-imaging-probe stripping cycles, each round uses a set of fluorescently labeled probes to generate a unique temporal barcode for each mRNA molecule.	reverse transcription → rolling circle amplification → *in situ* sequencing
Resolution	Subcellular (~200 nm)	Subcellular (~200-300 nm)	Subcellular (~300-500 nm)
Detection sensitivity	Single-molecule level (directly labeling each RNA molecule)	Single-molecule level (direct labeling)	Ssingle-molecule level with signal amplification
Throughput and capture area	Capable of detecting 10,000-20,000 genes.	seqFISH+: ~24,000 genes, but with imaging time spanning several days	Capable of detecting hundreds to a thousand genes.
Tissue compatibility	Best suited for fresh-frozen tissue; poor performance on FFPE; 3D imaging requires combination with tissue clearing.	Similar to MERFISH	Compatible with both fresh-frozen and fixed tissues; when combined with tissue clearing (for example, ExSeq + CLARITY), enables high-quality 3D imaging.
Analytical assumptions	Hamming distance-based error. correction, assuming that the error probability in each hybridization round is independent and known	Early seqFISH had no error correction; seqFISH+ employs combinatorial barcoding and enables partial error correction.	It relies on the sequential reading of fluorescent signals across sequencing rounds, assuming that the RCA products remain intact and the signal does not attenuate throughout the entire sequencing process.

MERFISH, multiplexed error-robust fluorescence *in situ* hybridization; seqFISH, sequential fluorescence *in situ* hybridization; ISS, *in situ* sequencing; RCA, rolling circle amplification; FFPE, formalin-fixed and paraffin-embedded.

However, spatial resolution has largely been confined to two-dimensional tissue sections, even though the structure and distribution of cells and molecules within tissues are three-dimensional. The recent emergence of tissue clearing techniques, which render intact tissues or even whole organisms optically transparent, has gradually made three-dimensional immunofluorescence imaging a reality. Existing tissue clearing-based three-dimensional immunostaining techniques fall into three categories: Solvent-based clearing (34-36), aqueous-based clearing (37-40) and hydrogel-based clearing (41-44). The rapid development of tissue clearing technologies enables the application of imaging-based ST to three-dimensional tissues and organs, as demonstrated by techniques such as ExSeq combined with CLARITY and smHCR combined with PACT.

The aforementioned imaging-based technologies also exhibit notable differences in core performance parameters, which directly determine the robustness of biological conclusions across different research contexts (Table II). First, regarding transcript capture strategies, both MERFISH and SeqFISH rely on multi-round specific probe hybridization, whereas ISS depends on signal amplification via RCA. This makes ISS more sensitive to single-base mismatches (suitable for mutation detection), but RCA efficiency varies considerably among different RNAs, potentially introducing quantitative bias (45-48). Second, in terms of resolution, although all three claim subcellular resolution, the actual effective resolution is influenced by the diffraction limit of the imaging system and probe density: MERFISH typically requires an optical resolution of ~200 nm to resolve single molecules, whereas the RCA products of ISS can cause signal overlap in densely expressed regions, leading to gene misassignment errors (27,49,50). Third, regarding detection sensitivity, single-molecule FISH (smFISH) directly labels each RNA molecule and offers the highest theoretical sensitivity; ISS achieves signal amplification via RCA, enabling detection of low-abundance transcripts,

Table III. Comparison of sequencing-based and imaging-based spatial transcriptomics technologies.

Core performance parameters	Sequencing-based spatial transcriptomics technologies	Imaging-based spatial transcriptomics technologies
Basic principle	Encodes positional information from tissue sections into 'spatial barcodes', acquiring transcriptomic data via high-throughput sequencing.	Uses fluorescently labeled probes for *in situ* hybridization with target RNAs, directly localizing RNA molecules through microscopic imaging.
Representative technologies	10x Genomics Visium, Slide-Se, Stereo-seq	MERFISH, SeqFISH, STARmap
Resolution	Typically tens to hundreds of micrometers; Stereo-seq can achieve 500 nm.	Generally higher, often at subcellular level.
Detection area	Larger	Smaller
Spatial dimensions	Primarily focuses on 2D tissue sections.	Enables 3D imaging via tissue clearing techniques (for example, CLARITY, PACT).
Primary applications	Tumors, developmental biology, whole-transcriptome mapping of complex tissues.	Neuroscience, immune microenvironment, subcellular localization, validation of cellular communication.
Experimental workflow	Relatively standardized, highly commercialized, suitable for FFPE samples.	Relatively complex, requires multiple rounds of hybridization and imaging, with stringent equipment and operational requirements.
Scalability	Easily integrated with multi-omics approaches.	Can be combined with multimodal imaging, such as immunofluorescence.

STARmap, spatially-resolved transcript amplicon readout mapping; FFPE, formalin-fixed and paraffin-embedded.

but at the cost of higher background noise (51-53). Fourth, the trade-off between throughput and capture area is critical: MERFISH can cover ~1 cm^2 per experiment detecting thousands of genes, while the high-throughput version seqFISH+ can detect tens of thousands of genes but requires days of imaging time, limiting sample throughput (28). Fifth, in terms of tissue compatibility, multi-round hybridization technologies (MERFISH, SeqFISH) have stringent requirements for tissue autofluorescence and RNA preservation, performing poorly on FFPE samples; by contrast, the RCA products of ISS are more resistant to photobleaching and, when combined with tissue clearing, are better suited for three-dimensional imaging (for example, ExSeq+CLARITY) (54,55). Finally, differences in analytical assumptions are often overlooked: MERFISH relies on Hamming distance for barcode error correction, assuming that the error probability of each hybridization round is independent and known; whereas ISS decoding depends on sequential reading of fluorescent signals across sequencing rounds, assuming that amplification products remain intact throughout the entire sequencing process. If these assumptions are violated, MERFISH's error correction mechanism can still partially recover data, while ISS may produce false negatives due to base deletions (27,56,57).

In summary, the choice of ST technology depends on the specific research objectives. Sequencing-based technologies enable whole-transcriptome profiling and are suitable for studying complex tissues such as tumors. Imaging-based technologies generally offer higher resolution and are primarily applied at the single-cell or subcellular level for predefined gene panels rather than whole-transcriptome analysis (Table III). Notably, with continuous technological advancements in recent years, novel technologies capable of combining large fields of view with high resolution have become feasible.

In practice, ST is often used in combination with scRNA-seq. ScRNA-seq sequences individual cells from dissociated tissues, allowing for high-precision identification of all cell types and subtypes present within a tissue through unsupervised clustering and the expression of known marker genes (58). Computational deconvolution algorithms (such as Cell2location, SPOTlight and Tangram) (59-61) can integrate scRNA-seq and ST data, enabling high-throughput mapping of cell types and signaling within tissues, thus generating comprehensive cellular atlases. For instance, this approach allows visualization of the spatial enrichment of different immune and stromal cells within tumor tissues (62). ScRNA-seq data can also be used with computational tools (such as CellPhoneDB, NicheNet and ICELLNET) to predict potential cell-cell communication (CCC) mediated by ligand-receptor (L-R) interactions (63-66). ST can then validate whether these predicted interactions indeed occur between physically adjacent cells. Integrating both approaches facilitates the robust reconstruction of cell communication networks within their spatial context (67).

From initial bulk sequencing techniques, which could only determine average molecular signals from large, heterogeneous cell populations, to single-cell sequencing, which enabled the revelation of unique molecular profiles of individual cells and further to spatial single-cell omics, which allows the resolution of gene expression programs and cell-cell interactions among heterogeneous cells in different regions of a tissue or organ, or among homogeneous cells executing biological processes, the rapid advancement of spatial omics technologies has led

to a more comprehensive and profound understanding of cellular functions in physiological, pathological, aging and apoptotic processes (68,69). Over the years, the resolution of ST technologies has continuously improved, evolving from the initial hundred-micrometer scale (Visium) to single-cell and even subcellular levels (Stereo-seq, MERFISH). Concurrently, the continuous development and optimization of data analysis methods, along with the integration of artificial intelligence technologies such as deep learning models, have enabled ST to integrate multi-level information from single-cell sequencing, proteomics and other modalities, providing richer data support for investigating tissue microenvironments, cell-cell interactions and disease progression. The TME is key for tumor initiation and progression. ST offers unique advantages for studying the TME, and research in this area has advanced rapidly (70,71).

3. Spatial dissection of the immune microenvironment during tumor progression

The tumor immune microenvironment is a dynamic and complex ecosystem composed of tumor cells, immune cells, cancer-associated fibroblasts (CAFs), vascular endothelial cells and extracellular matrix, among other components (2). During tumor initiation and progression, the tumor immune microenvironment serves not only as the supportive niche for tumor cell survival but also as a key site for immune evasion. Its composition is characterized not merely by cellular diversity, but more importantly by pronounced spatial heterogeneity in anatomical distribution (72). The emergence of ST has enabled *in situ* dissection of this spatial heterogeneity, revealing how stromal components restrict immune cell infiltration by constructing physical and chemical barriers, how immune cells undergo functional exhaustion within specific niches and why TLSs play diametrically opposite roles in different contexts (5,73). Such spatial information is pivotal in transforming the tumor immune microenvironment from a mere 'cell inventory' into a 'functional map', and it provides direct spatial targets for precision intervention.

Premalignant niches. ST enables the identification, at the very earliest stages of tumorigenesis, of spatial niche features that portend future immune escape and malignant progression and it reveals the spatiotemporal evolutionary patterns of premalignant lesions across multiple cancer types. In esophageal squamous cell carcinoma, single-cell ST has generated the first single-cell-resolution spatiotemporal dynamic atlas of multistage esophageal carcinogenesis (74), thereby surpassing the traditional linear evolution model and giving rise to a theoretical framework of 'spatial evolution of carcinogenesis'. To the best of our knowledge, this previous study (74) was the first to uncover that CAFs and invasive epithelial cells can form a key CAF-epithelial interactive niche (CAF-Epi niche) at the premalignant stage, which may serve as an important predictor of premalignant progression risk across several squamous cell carcinomas. In lung adenocarcinoma (LUAD), ST reveals that $KRT8^+$ alveolar intermediate cells represent temporal and clonal precursors to recognizable premalignant lesions; these cells are highly sensitive to IL-1β and other inflammatory signals and drive tumor initiation at the premalignant stage. This niche is highly active in early lesions but attenuates in invasive LUAD, suggesting that targeting therapy in conjunction with immunotherapy may offer an effective strategy for early-stage LUAD (75). Moreover, the interplay between KRAS mutation and p53 inactivation can sculpt a 'progenitor-like' microenvironment. ST confirms that this state interacts with surrounding stromal and immune cells to form a self-reinforcing 'premalignant niche', and that targeting KRAS or restoring p53 function can dismantle this niche (76). Temporal analyses further demonstrate a sequential process of 'fibrosis first, then immune remodeling' during early LUAD carcinogenesis: fibroblast reprogramming precedes macrophage expansion, with fibrotic signaling biased toward the tumor core and inflammatory fibroblasts enriched at the periphery (77). In gastric cancer, ST combined with single-cell sequencing constructs a high-resolution spatiotemporal atlas spanning normal gastric mucosa, gastritis and gastric cancer. This reveals a trajectory of mature chief cells transitioning into cancer stem cells (CSCs) accompanied by activation of EGFR and WNT pathways; CSCs, together with $CXCL13^+$ T cells, $CCL18^+$ M2 macrophages and inflammatory CAFs (iCAFs), constitute a CSC niche that drives tumor progression (78). Another study further identifies an NAD-dependent immunosuppressive microenvironment as a key driver of early intestinal-type gastric carcinogenesis: the AREG/NAMPT dual pathway promotes malignant transformation by activating macrophages and fibroblasts, and blockade of this pathway can inhibit the progression of premalignant lesions (79). Collectively, these studies demonstrate that, the premalignant niches exhibit context-dependent variation in cellular composition and driving signals across cancer types and ST enables researchers to directly localize and validate these rare and dynamic premalignant niches within native tissue, thereby providing precise spatial targets for early intervention.

Locally advanced stage. The locally advanced stage of tumors is a key phase in which tumors transition from *in situ* lesions to an invasive phenotype, accompanied by spatial remodeling and functional dysregulation of the immune microenvironment (80,81). During this stage, tumor cells, infiltrating immune cells and stromal cells form complex interaction networks within specific spatial compartments, collectively driving key events such as immune evasion, T cell exhaustion and immune exclusion (81,82). ST overcomes the limitations of conventional dissociation-based techniques and resolves *in situ*, within native tissue, the dual functionality of TLSs, the spatially heterogeneous niches of CAFs, the local drivers of T cell exhaustion and the molecular composition of immune exclusion barriers.

TLS. TLSs are ectopic lymphoid aggregates that form in non-lymphoid tissues under pathological conditions such as tumors, and they are primarily composed of B cells, T cells and dendritic cells (83). The application of ST enables precise dissection of the spatial localization, internal cellular composition of TLSs and their interactions with the surrounding microenvironment, thus revealing for the first time the mechanisms by which TLSs exert a dual role in antitumor immunity.

The antitumor function of TLSs is closely associated with their maturation status and spatial location. A recent pan-cancer

spatial atlas analysis of TLSs across 12 cancer types reveals that TLS maturation is accompanied by B cell differentiation, plasma cell dissemination, Tfh cell enrichment and enhanced interferon signaling. Moreover, a distance-dependent tumor signaling gradient exists around intratumoral TLSs: Tumor regions proximal to TLSs are enriched in immune activation pathways, whereas regions distal to TLSs are enriched in proliferation and invasion pathways (84). In prostate cancer, a previous study (85) clearly showed that intratumoral TLSs are not only more abundant but also more prone to form mature structures with germinal centers, and their presence is an independent protective factor for disease-free survival. By contrast, peritumoral TLSs are predominantly immature aggregates with loose architecture. In hepatocellular carcinoma (HCC), high-resolution ST combined with pseudotime analysis enables precise classification of TLSs into mature, maturation-prone and functionally deviated subtypes, among which mature and maturation-prone TLSs are notably associated with favorable prognosis and positive response to immune checkpoint blockade (ICB) (86). In renal cell carcinoma (RCC), TLSs are found to serve as sites where B cells undergo clonal diversification, selection and expansion, and the resulting plasma cells secrete IgG antibodies that directly induce tumor cell apoptosis. The B cell maturation trajectories within TLSs revealed by ST suggest that strategies aimed at inducing TLS formation or enhancing TLS function may improve ICB efficacy (87). In head and neck squamous cell carcinoma (HNSCC), mature TLSs are also associated with superior response to ICB therapy (87). Collectively, these cross-cancer studies consistently demonstrate that the antitumor function of TLSs is broadly conserved, and targeting TLS maturation pathways may represent a universal strategy for potentiating antitumor immunity.

Specific stromal cell subsets can actively promote TLS formation. In nasopharyngeal carcinoma, a population of $CXCL13^+$ CAFs has been shown to actively recruit B cells and promote their activation and antibody production by secreting CXCL13 and providing TNFSF13B-mediated maturation signals (88). In colorectal cancer (CRC) liver metastases, $CCL19^+$ fibroblasts are identified as key players that facilitate TLS formation and enhance antitumor IgG responses (89). These findings suggest that the TLS-promoting function of CAFs may be broadly conserved across cancer types, and that targeting CAFs to reconstitute a TLS-supportive microenvironment could emerge as a novel adjunct to immunotherapy.

The immunosuppressive functions of TLSs exhibit pronounced cancer-type specificity and can be driven by distinct metabolic or transcriptional programs. In high-grade serous ovarian cancer (HGSOC), Xu *et al* (90) explicitly associates 'dysmorphic TLS-like aggregates' with early patient relapse. Additionally, structurally mature TLSs (mTLSs) are associated with poor prognosis in HGSOC. Mechanistically, the study demonstrates that the presence of mTLSs associates with a reduction in follicular helper T cells within the TME, which biases $CD8^+$ T cell differentiation toward a terminally exhausted ($TIM\text{-}3^+PD\text{-}1^+$) phenotype rather than a stem-like exhausted ($TCF\text{-}1^+PD\text{-}1^+$) phenotype (87). This finding cautions that simply increasing TLS abundance in HGSOC may be insufficient to improve prognosis and could even be detrimental; combined strategies that target Tfh cells or employ anti-TIM-3 antibodies may be required to reverse terminal exhaustion. Similar phenomena have not been reported in HCC or RCC, suggesting that the immunosuppressive roles of TLSs may be highly dependent on the unique immune microenvironmental context of ovarian cancer. In a study of HCC (86), ST identified a subset of 'functionally deviated TLSs' in which intratumoral B cells display aberrant activation of tryptophan metabolism (high IDO1 and TDO2 expression), thereby creating a localized immunosuppressive milieu within the TLS. In clear cell RCC (ccRCC), the mechanism underlying TLS dysfunction is the aberrant enrichment of the transcription factor IRF4, which is associated with an immature TLS phenotype (91). Collectively, these findings indicate that although functionally deviated TLSs may exist across multiple tumor types, the underlying molecular mechanisms remain context-dependent.

ST has elevated TLS from a static, binary biomarker to a complex immune entity that must be functionally evaluated across multiple dimensions, structural, spatial, metabolic, transcriptional and cellular composition, thereby guiding the design of targeted intervention strategies.

CAF associated niches. CAFs represent a key stromal cell population within the TME characterized by pronounced heterogeneity. The rise of ST makes it possible, for the first time, to redefine their functional subtypes and identify targetable CAF subpopulations based on their spatial localization, molecular signatures and interactions with neighboring cells in native tissue contexts.

The spatial compartmentalization of CAF functional subtypes appears to be a conserved feature across cancer types. In HCC, $VEGFA^+$ CAFs are enriched in the tumor core, where they promote immunosuppressive angiogenesis through spatially adjacent vascular endothelial cells (92). In pancreatic ductal adenocarcinoma (PDAC), myofibroblastic CAFs (myCAFs) are closely juxtaposed with tumor cells and directly sequester immune cells, whereas iCAFs reside farther from the tumor center and shape an immunosuppressive environment (93). In oral squamous cell carcinoma, epithelial cells in highly metabolic tumor regions secrete lactate, which induces iCAF conversion and subsequently activates the HIF1α-CXCL12 axis to recruit regulatory T cells (Tregs) (94). In HNSCC, MHC-Ihigh Galectin-9+ CAFs construct a spatially defined 'barrier zone' that excludes and exhausts $CD8^+$ T cells through the upregulation of chemokines and Galectin-9 (95). Although these studies span different cancer types, ST analyses collectively reveal a general principle: the spatial distribution of CAF subtypes is not random; rather, they form specific spatial organizational patterns with the invasive front, perivascular regions or immune cell-enriched areas.

The upstream signals and functional outputs that drive CAF spatial heterogeneity vary considerably across cancer types. In glioblastoma (GBM), Jain *et al* (96) integrate scRNA-seq and ST to identify a CAF subpopulation highly expressing PDGF and TGF-β, whose primary function is to enhance immunosuppression by promoting the enrichment of CSCs and M2 polarization of macrophages. This mechanism is particularly prominent in GBM, but whether it plays an equally key role in other solid tumors remains unclear. In melanoma, $GDF15^+$ CAFs activate the GFRAL/RET axis on tumor cells through

paracrine signaling, thereby inducing macrophage M2 polarization (97); in cervical cancer, a COL14A1^{+}VIM^{+} CAF subpopulation interacts with tumor cells via the MDK-SDC1 pathway and is notably associated with T cell exclusion (4). These distinct ligand-receptor pairs, uncovered through ST combined with single-cell sequencing and other approaches, indicate that the molecular pathways by which CAFs mediate immune escape are highly context-dependent.

Through ST, the association between CAF spatial distribution and immunotherapy response is reported in multiple cancer types, yet its generalizability as a biomarker remains to be validated. In non-small cell lung cancer (NSCLC), patients who respond to neoadjuvant immunotherapy exhibit spatially organized units at the tumor margin comprising antigen-presenting CAFs, SELENOP^{+} macrophages and CD4^{+} T cells that promote immune activation (98). In HGSOC, the spatial organization pattern of tumor-associated CAFs with tertiary lymphoid structure-like aggregates is associated with early relapse (90). In cervical squamous cell carcinoma, POSTN expression, a functional indicator of myCAFs, is markedly lower in the drug-sensitive group than in the drug-resistant group (99). These findings suggest that CAF spatial configurations may serve as predictive biomarkers; however, the specific marker combinations vary across cancer types and require independent validation in each.

ST leads to the realization that CAFs, functioning as key orchestrators within the TME, display extensive spatial heterogeneity and functional plasticity. However, the exact molecular mechanisms and biomarkers are strongly dependent on the cancer type, which necessitates independent validation and the selection of tailored CAF-targeted strategies for each cancer context.

T cell exhaustion niches. T cell exhaustion represents one of the core mechanisms of immune evasion in locally advanced tumors. The application of ST enables the localization of exhausted T cell aggregates and the identification of their spatially proximal relationships with specific tumor cell subpopulations or stromal cells.

Spatial associations between exhausted T cells and specific myeloid or malignant cell subpopulations are reported across multiple tumor types. In primary central nervous system lymphoma, T cell exhaustion markers are spatially associated with a malignant B cell subpopulation that highly expresses multiple chemokines and immune checkpoint ligands (100). In HCC, regions enriched with exhausted T cells concurrently exhibit high expression of the M2 macrophage marker CD163 and the CAF marker VIM (101). In ccRCC, exhausted T cells are preferentially located within the tumor interior, and the uneven distribution of the same T cell clones across different tumor regions suggests that the local microenvironment shapes T cell status and expansion (102). In breast cancer, exhausted T cells predominantly aggregate in regions with immature TLS and are associated with the spatial distribution of CXCL13^{+} T cells (103). These cross-cancer ST studies collectively support a general conclusion: T cell exhaustion is not a cell-autonomous process but is driven by the spatial architecture of the local microenvironment.

Studies find that the key stromal cell types driving T cell exhaustion may differ across cancer types. Xun *et al* (104) performed ST analyses across multiple cancer types (breast cancer, CRC, ovarian cancer and ccRCC) and found that exhausted CD8^{+} T cells and ALCAM^{high} macrophages are highly enriched at the tumor boundary, with co-localized Tex cells exhibiting higher exhaustion scores. This phenomenon is observed across multiple types of cancer, suggesting that ALCAM^{high} macrophages may represent a cross-cancer driver of exhaustion. However, in a study of ovarian cancer chemotherapy (105), T cell exhaustion was shown to be driven primarily by chemotherapy-induced myeloid cell networks (Myelonets) rather than by pre-existing macrophage subpopulations, indicating that the driving mechanisms of T cell exhaustion can be reshaped in the context of treatment. In GBM, the spatial distribution of T cell exhaustion is also closely associated with hypoxia signaling (106); this feature may be particularly prominent in the highly hypoxic GBM microenvironment, while it may not dominate in other tumors with improved oxygenation.

These ST-based findings suggest that reversing T cell exhaustion represents a key strategy in immunotherapy; however, the selection of spatial targets must be tailored to the cancer type and the treatment context. In ovarian cancer undergoing chemotherapy, ST reveals that chemotherapy-induced myeloid cell networks form an immunosuppressive microenvironment that drives functional exhaustion of CD8^{+} T cells, thereby promoting chemoresistance (105). This finding indicates that co-targeting myeloid cells may be an effective strategy to reverse exhaustion in ovarian cancer, whereas in other cancer types, targeting CAFs or specific macrophage subpopulations may be required. ST enables the identification of spatial drivers of T cell exhaustion across various cancer types and treatment settings, thus providing a logical basis for precision combination therapy.

Immune exclusion niches. Among the most direct contributions of ST is the elucidation and definition of 'immune exclusion niches', the phenomenon by which cytotoxic T cells are actively excluded from the tumor core.

CAF subpopulations enriched in extracellular matrix components (ECM-CAFs) mediate immune exclusion is conserved across multiple cancer types. A pan-cancer study integrating 16 cancer types reveals that ECM-CAFs are specifically enriched at the tumor boundary. These ECM-CAFs not only form a physical barrier that impedes T cell infiltration but also directly induce T cell exhaustion by highly expressing LGALS9, TIM-3 and other immune checkpoint ligands. In patients with HCC who are non-responsive to immunotherapy, the enrichment of ECM-CAFs is notably associated with a spatial distribution pattern in which T cells are confined to the tumor periphery, thereby providing solid clinical evidence for the concept of a 'spatial immune barrier' (107). Similar immune exclusion patterns are also observed in triple-negative breast cancer and high-grade serous ovarian cancer (108,109). This cross-cancer and cross-platform evidence suggests that ECM-CAF-mediated immune exclusion represents a prevalent immune evasion mechanism.

The specific molecular features and spatial organization patterns of immune exclusion are modulated by local microenvironmental factors. In GBM, integrated ST and spatial proteomic analyses reveal that mesenchymal-like tumor cell

states are tightly organized with macrophages and T cells into specific multicellular units, and this spatial organization is governed predominantly by hypoxic signaling (106). In GBM, hypoxia is a key driver of immune exclusion; however, in well-oxygenated tumors such as renal cancer, hypoxia may not be a major contributing factor. Furthermore, in triple-negative breast cancer, immune exclusion is associated with the spatially restricted activation of the TGF-β signaling pathway (109), while in ovarian cancer, immune exclusion is associated with specific CAF subpopulations (108). These differences indicate that, while immune exclusion is a prevalent phenomenon, its upstream driving signals and specific spatial organization patterns are highly context-dependent.

ST is what converts immune exclusion from a descriptive concept into a targetable entity, jointly characterized by specific cell subsets, particular molecular pathways and defined spatial locations.

Distant metastasis stage. Distant metastasis is one of the leading causes of cancer mortality. Its occurrence depends on the ability of tumor cells, after detaching from the primary site, to successfully adapt to and remodel the microenvironment of distant organs (81,110,111). The application of ST enables the direct *in situ* investigation of two key steps in the metastatic process: The pre-conditioning of the pre-metastatic niche and the dynamic remodeling of the tumor invasion front (5,75). ST allows researchers to visualize, across different cancer types and metastatic organs, the microenvironmental differences between primary and metastatic lesions, the spatial propagation characteristics of immunosuppressive cellular neighborhoods and the spatial coupling mechanisms of epithelial-mesenchymal transition (EMT) and immune escape at the invasion front (94,112-114), thereby elevating metastasis research from a 'molecular inventory' to the level of a 'spatial evolutionary atlas'.

Pre-metastatic niche. In recent years, advances in ST have opened new avenues for understanding tumor evolution and metastatic mechanisms from a spatial dimension. In CRC liver metastasis, ST reveals that $CCL19^+$ fibroblasts form specific spatial structures in the liver that promote TLS formation and antitumor IgG responses, and the absence of this niche is associated with metastatic progression (89). In PDAC, ST comparison of primary and metastatic lesions reveals marked alterations in the spatial distribution patterns of iCAFs and myCAFs at metastatic sites relative to primary tumors (115). Spatial proteomic analysis of lymph node metastases further demonstrates that, although lymph node metastases retain lymphoid structures composed of B cells, $CD4^+$ T cells and other immune cells, they exhibit pronounced abnormalities in functional markers: T cells highly express PD-1 and LAG-3, Tregs display an activated state with elevated Ki67, ICOS and IL-10, and myeloid cells and CAFs show upregulated PD-L1 and IL-10 expression. Importantly, spatial neighborhood analysis identifies a 'myeloid/CAF-enriched cellular neighborhood' that is enriched not only within metastases but can also be traced into adjacent uninvolved tumor regions, suggesting that immunosuppression can propagate spatially (116). In a multi-organ metastasis study of PDAC, integrated ST and single-cell imaging reveals that metastases do not simply recapitulate primary tumor features; instead, they adapt to the local microenvironment through organ-specific clonal selection and lineage remodeling. Liver metastases manifest an immune exclusion niche dominated by a basal-like phenotype, whereas lung metastases display a classical phenotype with a relatively active immune microenvironment, highlighting the substantial transcriptomic heterogeneity and dynamic microenvironmental changes during pancreatic cancer metastasis (93). A study using high-resolution single-cell ST (CosMx SMI) on SCLC systematically constructs a spatial cell atlas of primary tumors and lymph node metastases, revealing from a spatial dimension the heterogeneous evolution of the TME and the remodeling of cellular interactions during SCLC lymph node metastasis (117).

These studies collectively demonstrate that ST enables visualization of the microenvironmental differences between primary and metastatic sites across different cancer types and metastatic organs, as well as the spatial propagation characteristics of immunosuppressive cellular neighborhoods. However, it remains unclear whether these findings are generalizable to other types of pre-metastatic niches. The molecular features of pre-metastatic niches are highly dependent on the primary tumor type and the tissue context of the metastatic target organ. Therefore, further cross-cancer and cross-metastatic organ comparative studies are required to extract universally instructive principles of metastatic evolution from this context dependency. Such cross-organ and cross-cancer comparisons are made possible by ST, which in turn provides spatial targets for precision intervention against the metastatic microenvironment.

Tumor invasion front. The tumor invasion front is a dynamic zone at the interface between the primary tumor and the surrounding stroma, representing the most active site of EMT, tumor cell invasion and the establishment of an immunosuppressive microenvironment.

An EMT signature is enriched at the tumor-stroma boundary across multiple cancer types rather than being uniformly distributed throughout the tumor. In HCC, high-resolution Stereo-seq technology precisely delineates an invasion zone ~500 μm wide at the tumor boundary, within which tumor cells exhibit pronounced EMT signatures, metabolic reprogramming and molecular hallmarks of immune escape (118). In gastric cancer, spatial atlases reveal that the tumor margin (G2-enriched region) displays higher activity of EMT and angiogenesis pathways compared with the tumor core (G1-enriched region) (119). In CRC, the deep learning algorithm GASTON identifies type II genes that predominantly describe the upregulation of EMT genes outside the tumor boundary (120). Collectively, these independent studies across diverse cancer types consistently demonstrate that the tumor-stroma interface serves as a spatial hub for EMT, a broadly conserved principle.

The specific stromal cell subsets and signaling pathways that drive EMT vary across cancer types. In CRC, studies reveal that distinct CAF subpopulations spatially promote EMT through different signaling axes. Yang *et al* (121) find that malignant epithelial cells in metastatic CRC can undergo EMT to transdifferentiate into $CXCL1^+$ CAFs, a process driven by the transcription factor BHLHE40; Lu *et al* (122) identify

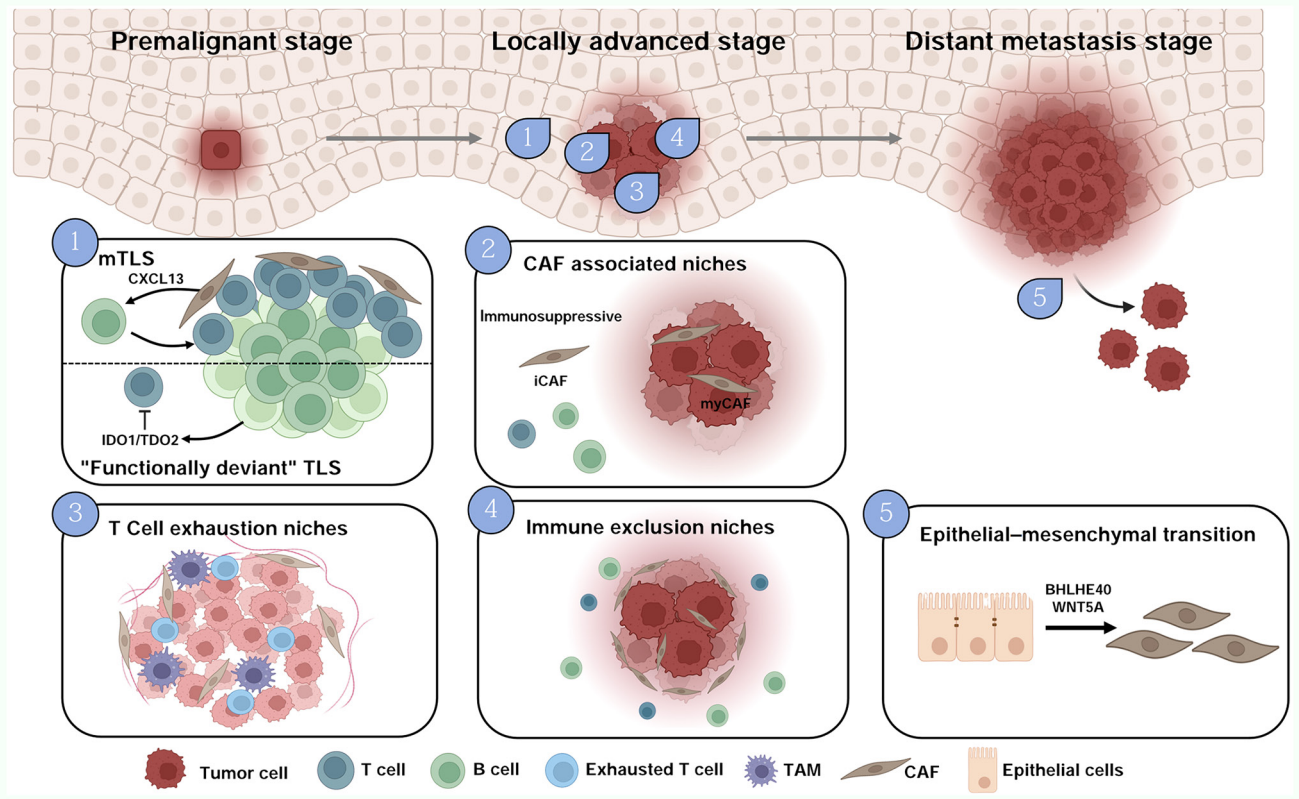

Figure 1. Typical cellular composition and organization of five biologically important spatial niches within the tumor microenvironment across the course of tumor progression. The figure summarizes the major spatially defined niches in the tumor immune microenvironment across premalignant, locally advanced and metastatic stages. In the locally advanced stage: TLSs exhibit dual functions; mTLSs promote antitumor immunity via B cell differentiation and plasma cell dissemination (for example, CXCL13$^+$ CAFs recruit B cells and enhance antibody production), while functionally deviated TLSs (for example, those with IDO1/TDO2 upregulation in HCC) create immunosuppressive milieus. CAF-associated niches are spatially compartmentalized into distinct subtypes. The myCAFs localize adjacent to tumor cells, whereas iCAFs are positioned distantly; specific CAF subsets further express distinct ligand-receptor pairs. T cell exhaustion niches are characterized by spatial association of exhausted CD8$^+$ T cells with M2-like TAMs. Immune exclusion niches are defined by ECM-CAFs that form physical barriers. In the distant metastasis stage: At the tumor invasion front, EMT is enriched and driven by distinct CAF subsets (for example, CXCL1$^+$ CAFs via BHLHE40 or CTHRC1$^+$ fibroblasts via WNT5A). Spatial transcriptomics enables the in situ resolution of these niches, transforming descriptive patterns into testable spatial hypotheses and potential therapeutic targets. TLS, tertiary lymphoid structures; mTLS, mature TLS; CAF, cancer-associated fibroblast; iCAF, inflammatory CAF; myCAF, myofibroblastic CAF; HCC, hepatocellular carcinoma; TAM, tumor-associated macrophage; ECM, extracellular matrix; EMT, epithelial-mesenchymal transition.

a distinct population of CTHRC1$^+$ fibroblasts that secrete WNT5A to form a spatially adjacent pro-EMT niche with malignant epithelial cell. In GBM, M2-like tumor-associated macrophages (TAMs) are predominantly distributed at the tumor invasion front and exhibit a significant spatial association with mesenchymal-like tumor cell states, implicating them in the construction of an immunosuppressive barrier at the tumor boundary (96). In acral melanoma, tumor cells with high EMT signatures are spatially co-enriched with APOE$^+$/CD163$^+$ TAMs and promote tumor invasion through IGF1-IGF1R signaling (123). In ccRCC, the EMT signatures in metabolically active regions are associated with sphingolipid metabolic reprogramming in M2 macrophages (124). These differences indicate that, although the spatial localization of EMT is universal, the specific modes of interaction with microenvironmental cells are highly context-dependent.

ST enables the redefinition of EMT, transforming it from a purely tumor-cell-intrinsic phenotypic program into an 'invasion front niche', a niche that is jointly orchestrated by a specific spatial location, specific stromal cell subsets and a specific metabolic microenvironment, and that functions simultaneously in invasion and immune exclusion. Fig. 1 illustrates the typical cellular composition and organization of five biologically important spatial niches within the TME across the course of tumor progression.

4. Toward clinical application: Limitations and breakthroughs in spatial transcriptomics technology

Conventional clinical diagnosis and treatment rely on imaging and histopathology as adjunct tools, yet often overlook the spatial cellular phenotypes underlying histopathological findings. The finer-resolution molecular insights offered by ST enable more precise disease stratification, outcome prediction and assessment of therapeutic response. Notable progress has been made in oncology, where spatial molecular landscapes have been shown to associate with tumor growth, susceptibility to metastasis and efficacy of immunotherapy. These discoveries highlight the clinical potential of spatial biomarkers, providing actionable insights for precision medicine. However, before ST can be effectively integrated into routine clinical diagnosis and decision-making, several key technical challenges must be addressed, including limited resolution, sample constraints, algorithmic bias and lack of cross-platform

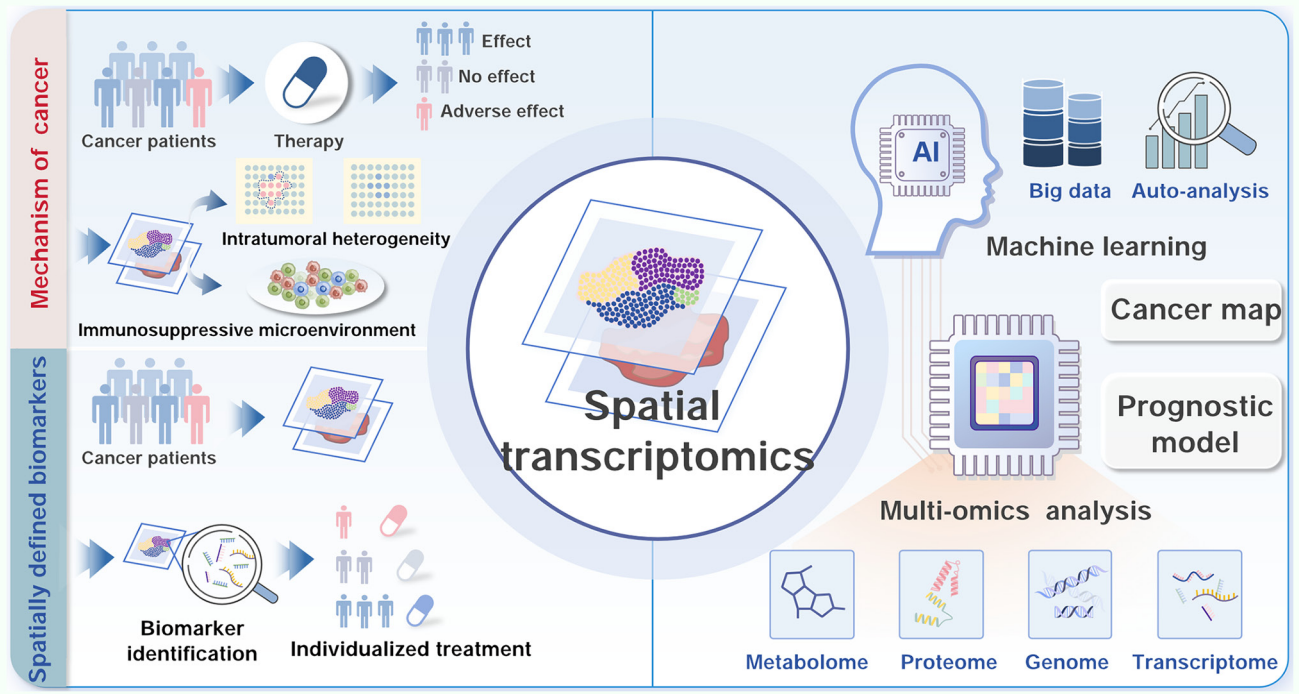

Figure 2. Spatial transcriptomics play multiple roles in advancing the precision and personalization of tumor immunotherapy. For patients resistant to immunotherapy, these technologies enable the exploration of tumor heterogeneity and the immunosuppressive microenvironment, identify distinct gene expression features and facilitate the efficient development of novel drug targets. They also aid in the development and validation of tumor biomarkers, guiding personalized treatment strategies. Furthermore, by integrating multi-omics analytical platforms and machine learning techniques, spatial transcriptomics are driving a shift in biomarker screening from single-marker development to the establishment of multi-parameter predictive models. Simultaneously, they contribute to the construction of more comprehensive tumor atlases, reshaping the scientific understanding of tumor biology.

standardization. There is an urgent need to establish widely accepted standardized operating procedures covering sample collection, platform testing and data analysis. The rapid development and maturation of machine learning in recent years have created new opportunities to address these technical bottlenecks (11). Looking ahead, as omics technologies and machine learning become increasingly integrated, advances in multimodal data integration and three-dimensional tissue reconstruction will provide even more powerful technical support for deepening the understanding of tumor evolution and overcoming challenges in cancer therapy.

Clinical translational potential of spatial transcriptomics technology. The breakthroughs of ST in revealing cellular heterogeneity and decoding cell-cell interactions are driving the translation of related research toward clinical applications. In this context, the present review focuses on two key translational paths: First, the identification of spatially defined biomarkers for use in clinical diagnosis or subtyping; and second, the elucidation of mechanisms underlying therapeutic response to guide the discovery of new therapeutic targets (see Fig. 2).

First, ST technology, with its unique spatial resolution capability, holds a notable advantage in discovering novel spatially defined candidate biomarkers. From an ST perspective, the TME can be partitioned into multiple spatial domains, each characterized by consistent functional states or morphological components. Molecular expression profiles differ substantially across these domains, and CCC within the same domain are mediated by key L-R pairs. Biomarkers associated with tumor prognosis are often derived from differentially expressed molecules across distinct regions of the TME, reflecting divergent clinical outcomes. Chauvin *et al* (125) used the Xenium platform to perform ST analysis on tissue samples from human HGSOC. They found that, compared with tumor cell regions, stromal regions exhibited elevated FST and FSTL3 signaling in cancer-associated mesothelial cells and CAFs. Tumor models overexpressing FSTL3 displayed a more fibrotic microenvironment with reduced immune cell infiltration (125). Moreover, FSTL3 similarly influences tumor infiltration in CRC, gastric cancer and LUAD, underscoring its potential as a prognostic biomarker across multiple cancer types (126-128). Expanding biomarker screening beyond specific tumor types, the combination of single-cell RNA-seq and ST enables the resolution of single-cell gene expression within complex, highly structured tissues. It is well established that fibroblasts and macrophages are ubiquitous in the TME and engage in intensive CCC. The transferase SLFN11 is significantly downregulated in both cell types across most tumors, and multi-omics analyses suggest its association with DNA repair, the P53 pathway and tumor immunity. SLFN11 expression level thus holds great promise as a diagnostic biomarker and a predictive indicator of treatment efficacy (129). Furthermore, identified biomarker molecules can also guide the selection of clinical therapeutic agents in oncology. Wang *et al* (130) through ST sequencing and bulk RNA-seq analysis, provided the first evidence of the prognostic significance of an ADME-related prognostic signature in ccRCC and its potential application in guiding personalized treatment strategies. In summary, the integration of ST technology on one hand

provides direction for biomarker development, screening for differentially expressed molecules within specific spatial domains may improve discovery efficiency, and on the other hand, the wealth of omics data facilitates the combined development of multi-marker panels, further enhancing the predictive and discriminative power of biomarkers, supporting the construction of tumor prediction models and aligning with the advancement of precision medicine.

Second, ST can resolve the spatial context of disease initiation and progression, an unique perspective that facilitates the discovery of previously overlooked, spatially dependent novel therapeutic targets. Tumor development is characterized by multiple stages and steps, and intratumoral heterogeneity (ITH) leads to regional differences in immune status and drug sensitivity. Conventional bulk sequencing masks this spatial complexity, whereas ST preserves tissue architecture while revealing tumor heterogeneity patterns, positioning it as a key technology to address this challenge. Zhang *et al* (131) used ST analysis to show that in regions of HCC responsive to cabozantinib and nivolumab (CABO/NIVO) combination therapy, PAX5 is localized to immune areas adjacent to tumor clusters, indicating a B cell-driven active immune state. By contrast, within tumor-CAF interaction zones, ECM remodeling genes are activated, forming a drug-resistant niche with sparse immune infiltration. Qin *et al* (132) identified four tumor cell subpopulations in pancreatic cancer and found that crosstalk between RPS4Y1+ tumor cells, fibroblasts, and CD8+ T cells promotes immunosuppression. Song *et al* (133) demonstrated in non-SCLC that PD-L1 expression in the stromal region has stronger predictive power for bispecific antibody response, and that integrating DSP with multiplex immunofluorescence improved research efficiency. ST-based dissection of ITH can guide the development of prognostic indicators and novel therapeutic targets. Mao *et al* (134) found that regions with low MC content colocalize with CAF genes and exhibit minimal immune infiltration, and that MC heterogeneity promotes immune evasion in HCC, with relevant gene signatures serving as prognostic markers. Guo *et al* (135) observed in MMRd endometrial cancer that immune features in tumor-enriched regions align with CD8+ T cell infiltration and identified potential biomarkers including HLA class I and DNMT3A. ST technology provides direct visualization of cellular distribution and communication across distinct niches, offering tissue- and molecular-level evidence for understanding immunotherapy sensitivity and resistance, and holds promise for identifying new therapeutic targets.

The highly immunosuppressive TME is a major contributor to drug resistance in solid tumors. In recent years, researchers have increasingly combined ST with technologies such as CODEX and single-cell sequencing to dynamically monitor immune cell infiltration and changes in gene expression. In the context of radiotherapy, which can promote antitumor immunity, Oyoshi *et al* (136) found that following radiotherapy, the infiltration of immune cells including T cells and B cells in the TME increased, with distinct expression patterns observed at different stages. In muscle-invasive bladder cancer, patients who achieved pathological complete response after neoadjuvant chemotherapy exhibited lower neutrophil counts and lower neutrophil-to-lymphocyte ratios, along with increased infiltration of B and T cells (137). Current research focuses on the contribution of specific immune cell subtypes to drug resistance, including macrophages, Tregs, CAFs and plasma cells (138). In GBM, the roles of distinct macrophage subtypes have received considerable attention. Liu *et al* (139) demonstrated that VSIG4+S100A10+ TAMs colocalize with T cells and suppress antitumor immunity. Gao *et al* (140) identified a novel MDM subtype with high TREM-1 expression in perinecrotic hypoxic regions and showed that targeting this subtype enhances chemosensitivity. In recurrent GBM, oligodendrocyte enrichment and microglial activation have been observed (141). In low-grade glioma, FN1+ TAMs are enriched in hypoxic regions and associated with recurrence (142). Similar phenomena have also been reported in CRC and metabolic dysfunction-associated steatohepatitis-related hepatocellular carcinoma, where such macrophages are typically localized to hypoxic niches and participate in immunosuppression. In HCC research, distinct CAF subtypes exert opposing effects: A Treg-CAF cluster at the tumor margin forms an immunosuppressive niche considered to drive immunotherapy resistance in steatohepatitic HCC (143), whereas the FMO2+ CAF subset is associated with improved prognosis following anti-PD-1 therapy (144). Collectively, ST compensates for the inability of conventional transcriptomics to resolve cellular spatial localization, providing a powerful tool for elucidating the mechanisms by which stromal cell subsets mediate immune evasion.

Key technical challenges constraining clinical application. Since the advent of ST technology, continuous iterative optimization to meet research and other application needs, along with advances in bioinformatics capabilities for spatial data analysis, has revealed complex intercellular spatial relationships within the TME. These insights are key for understanding tumor progression and treatment resistance, and demonstrate strong translational potential in the field of oncologic clinical therapy. However, before ST can be truly implemented in clinical practice, connecting spatial biomarkers to patient treatment outcomes and demonstrating their validity across different therapeutic settings will require overcoming a series of obstacles. The present review discusses key considerations that constrain the use of ST in clinical diagnosis and treatment, encompassing technical algorithms, sample selection and data validity validation.

Trade-off between resolution and coverage. The fundamental principles underlying sequencing-based and imaging-based methods inherently limit the resolution and coverage of sample detection. Next generation sequencing (NGS)-based ST platforms, represented by 10x Genomics Visium, rely on fixed spots with spatial coordinates to capture mRNA released from all cells within the corresponding region. Due to the physical size of individual spots, typically 10 to 100 mm, the data captured by each spot represents mixed transcriptional signals from multiple cells, precluding precise assignment to single cells and thus yielding lower resolution. By contrast, imaging-based ST platforms, represented by Xenium, CosMx and CODEX, are designed to acquire *in situ* data at single-molecule resolution, enabling RNA localization at the subcellular level (down to 100-200 nm) and retaining more intracellular information. However, these methods are limited

to fluorescence detection of predefined target genes, and detection efficiency decreases as panel size increases.

In clinical research, specific diagnostic and therapeutic needs place different emphasis on resolution vs. coverage, necessitating a deliberate trade-off. Sequencing-based methods enable unbiased capture of polyadenylated transcripts, allowing genome-wide investigation of gene expression. They are suitable for gaining a global understanding of tissue architecture, identifying novel cell subtypes, and revealing overall expression differences across distinct functional regions of tumor tissue. Additionally, the sequence information obtained through NGS can be used to detect somatic variants, transcript isoforms, non-coding genes and TCR/BCR clonotypes. Imaging-based methods, constrained by reliance on pre-designed probes, limit the number of target genes that can be measured on a single panel and cannot retrieve sequence information. However, subcellular-resolution platforms offer higher resolution, shorter turnaround times and greater interpretability of results, making them particularly well-suited for hypothesis validation and clinical testing. The high-resolution microscopy required for multi-round fluorescence capture renders imaging-based ST technologies more expensive than sequencing-based approaches, a significant factor limiting their clinical adoption. With ongoing technological iterations, sequencing-based methods are progressively moving toward higher resolution. The Stereo-seq spatial omics platform from BGI achieves nanoscale resolution through chip-arrayed DNBs. Future ST platforms are expected to combine both high resolution and broad coverage, making them more suitable for clinical applications.

Sample limitations. FFPE samples are a common method of tissue processing in clinical practice. Formaldehyde fixation preserves tissue and cellular morphology, and after dehydration and paraffin embedding, the tissue can be sectioned into slices of 5 μm or thinner for histologic and immunopathologic assessments required for diagnosis, while also allowing sample storage under non-frozen conditions. In medical practice worldwide, standardized protocols for the collection, preservation, sectioning and storage of FFPE samples have been systematically established. Due to the routine need for solid tumor diagnosis in clinical settings, hospitals have accumulated large repositories of such specimens, often accompanied by detailed clinical annotations, providing valuable resources for investigating tumor development and therapy (5,145). The ability of ST technologies to obtain accurate spatial expression information depends critically on the preservation of tissue morphology and RNA integrity. Because RNA is unstable at room temperature and highly prone to degradation, ST analysis requires sample fixation. Compared with other sample types, FFPE samples offer distinct advantages, including well-preserved spatial context and cellular architecture with minimal distortion, making them the current sample of choice for ST analysis. However, it is important to note that during the fixation process, formaldehyde crosslinks free molecular chains, which simultaneously leads to nucleic acid fragmentation and protein-nucleic acid crosslinking, ultimately resulting in samples that cannot provide high-quality RNA molecules for ST analysis (146). This represents a major factor limiting the application of FFPE samples in clinical ST analysis. By contrast, fresh frozen (FF) samples allow the acquisition of intact RNA molecules, but their preparation, transport, storage and processing require stringent conditions, including maintaining subzero temperatures to prevent RNA degradation (147,148). Moreover, clinical practice lacks standardized operating procedures to ensure consistency and quality control of FF samples. To improve RNA quality from such samples, Wulf *et al* (149) developed a novel miRNA sequencing strategy called CapTS-seq, which combines chemical capping and template switching to enhance miRNA library quality; however, this study did not address validation of detection efficiency related to ST technologies (149). Therefore, obtaining FFPE samples with high-quality RNA remains a challenge that must be addressed when advancing ST technologies for clinical tumor diagnosis and therapy.

Bioinformatics algorithmic bias. Regardless of whether spot-based or imaging-based platforms are used, the transcriptomic landscape that contains spatial information is often not directly visualized. This inevitably requires computational methods to model and annotate spatial data, indirectly reconstructing the complex distribution and expression states of tumor cells, immune cells and stromal cells within the TME under *in vivo* conditions (150-152). These computational approaches, such as cell segmentation and deconvolution, are essentially fitting procedures that approximate true spatial adjacency relationships rather than direct reflections of the real world. Consequently, algorithmic bias can readily lead to ST results with low reliability, thereby affecting downstream analyses.

Segmentation errors. RNA hybridization-based ST captures molecular and cellular features at subcellular resolution, yielding more accurate transcriptional mapping and cell phenotyping compared with sequencing-based platforms. This, however, places higher demands on the accuracy of segmenting image volumes into individual cells. Existing cell segmentation methods rely on structural markers (image staining-based segmentation) and transcript clustering to delineate individual cells. Approaches such as StarDist, CosMx and Xenium achieve segmentation through specific staining of cellular components (StarDist uses nuclear staining and expansion to generate pseudo-cell boundaries) (153). Segger models the spatial relationship between nuclei and surrounding transcripts to refine initial boundaries (154). These methods are limited by manual annotation, staining quality, sensitivity to cell density and mismatch with true transcriptomic profiles, making it still challenging to correctly assign individual molecules to their cells of origin. On one hand, tumor cells, immune cells and stromal cells within the TME exhibit distinct morphologies and highly variable spatial compositions, particularly in regions with high cell density, irregular morphology or tightly packed tissues such as the epithelial layer and tumor parenchyma, where under-segmentation or over-segmentation frequently occurs. On the other hand, parameter settings in segmentation algorithms also constrain performance; for example, the optimal parameters of DBSCAN are closely related to target cell size and transcript density (155). Erroneous assignment of RNA molecules from neighboring cells to the target cell leads to data contamination, which has been shown across multiple

tissues and platforms to affect downstream analyses such as false positives in differential expression and misinterpretation of cell-cell interactions. These effects often dominate analytical outcomes (156,157). To further improve the accuracy of segmentation-based computational methods, functional annotation of transcriptomes can be leveraged. JSTA incorporates prior knowledge of cell type-specific gene expression to achieve cell segmentation, improving RNA assignment accuracy by >45% (158). RedeFISH aligns segmented cell expression profiles with single-cell expression data to achieve optimal segmentation. cellAdmix effectively identifies and separates confounding data through matrix factorization of local molecular neighborhoods, thereby reducing its impact on downstream analyses (156). Furthermore, manual annotation and review remain necessary at this stage to address segmentation errors caused by tumor cell atypia (155).

Deconvolution uncertainty. Sequencing-based platforms provide spatially resolved gene expression data by sequencing RNA molecules captured within spots, but typically lack cellular resolution. Therefore, cell type deconvolution is required to infer the cellular composition of each spot (159,160). Current computational methods fall into two major categories: Supervised deconvolution and unsupervised deconvolution. Supervised deconvolution methods, represented by RCTD, SPOTlight, cell2Location, Tangram, CytoSpace and Spotiphy, utilize single-cell RNA-seq reference data and employ strategies such as regression models, Bayesian models and optimal transport mapping to infer the compositional proportions, counts or even single-cell localization of different cell types from the mixed expression signals of each spot. For such methods, the degree of alignment between the single-cell RNA-seq reference dataset and the ST data significantly affects deconvolution results. If a particular cell type is absent from the reference data, the deconvolution model will erroneously assign expression signals from the missing type to other related cell types, which is a major source of result bias. Furthermore, deconvolution outputs are typically cell type proportions, which are compositional data where the components sum to a constant (for example, 100%). This violates the independence assumption of conventional statistical methods such as linear regression, leading to spurious associations. Some Bayesian models address this by setting probabilistic priors for variables such as cell type proportions and gene signatures from reference data, updating these considerations using spatial data. The resulting posterior distributions provide interval estimates rather than point estimates for parameters, thereby effectively quantifying uncertainty. Unsupervised deconvolution methods, represented by CARD and SpiceMix, do not rely on external reference data. Instead, they automatically discover latent 'factors' from the statistical structure of the ST data alone using dimensionality reduction techniques such as matrix factorization, with the factors then manually annotated as cell types. In this process, the number of factors and their annotation depend on the researcher's subjective judgment. Matrix factorization algorithms are sensitive to initial values and data noise and different runs may yield different results. The resulting 'factors' may represent genuine biological cell types or may be technical noise subject to overinterpretation, representing a biological hypothesis that requires validation (101,161).

Batch effects. The clinical application of ST technology in oncology still requires overcoming challenges posed by batch effects. Batch effects arise from multiple factors including sample collection, processing conditions, sequencing platforms and variations in section geometry. If not properly adjusted, they may obscure true biological variation, leading to inaccurate downstream analyses. This issue is particularly pronounced in clinical data involving multiple patients, multiple institutions and diverse treatment histories. As a precursor to ST data, single-cell RNA-seq also suffers from batch effects and data variability. Correction strategies developed to date, such as Harmony, ComBat, fastMNN, Scanorama and Seurat-CCA, are based on shared embedding space analysis and neural network decoding, reducing noise and batch-specific artifacts while maximizing retention of true biological variation. However, directly applying batch correction tools designed for single-cell RNA-seq to ST data ignores spatial location information of cells, resulting in suboptimal performance (162). Although existing algorithms have begun to incorporate spatial features of ST data during batch effect removal, the complexity and non-specificity of spatial characteristics mean that no method has yet explicitly addressed this problem by integrating spatial information from gene distributions with gene expression features during batch effect correction (163,164).

Overinterpretation of L-R interactions. Deciphering CCC between adjacent cells is fundamental to understanding the coordination of cellular community behavior, tissue architecture and tumor-immune interactions within the TME. L-R interactions represent a key aspect of CCC research, as receptor activation can trigger intracellular signaling cascades that subsequently regulate cellular behavior. Advances in high-resolution sequencing technologies have greatly propelled the study of CCC using ST data. Nearly 50 L-R databases have emerged in this field, and these resources differ substantially in annotation quantity, species coverage, and signaling types. The choice of database largely influences analytical outcomes (165). The current mainstream strategy uses high-quality L-R databases as prior knowledge to align ST expression profiles with these databases for inferring potential cell-cell communication events. Tools such as Giotto, Squidpy, Spateo and CytoSignal provide modules that integrate L-R expression with spatial information to infer and quantify L-R communication scores (166-169), while COMMOT employs optimal transport theory to model cost-effective signaling molecule flow among spatially adjacent cell types (170). However, computational inference based on database alignment cannot be equated with actual biological processes. Even when ligand-expressing cells and receptor-expressing cells are spatially adjacent, this only indicates the possibility of CCC rather than established functional signal transmission, due to potential physical barriers or high RNA expression but low protein abundance (171). Furthermore, a strong L-R colocalization signal at a single time point cannot distinguish whether the signaling event has yet to initiate or has already terminated. In computational inference, these distinct scenarios are often uniformly classified as 'communication present', leading to overinterpretation of L-R interactions (171). Bridging the gap between computational

inference and actual biological processes ultimately depends on rigorous experimental validation.

Platform standardization and the translational gap. The rapid development of ST technologies has given rise to multiple detection platforms. However, technical heterogeneity across platforms poses serious challenges for data integration and comparison. Addressing cross-platform standardization is particularly key for advancing ST toward clinical diagnosis and precision medicine applications.

In recent years, several teams worldwide have attempted to establish standardized evaluation frameworks for ST platforms and have made considerable progress. You *et al* (172) systematically compared 11 sequencing-based platforms and, through the development of the cadasSTre dataset, identified molecular diffusion as a key parameter affecting effective resolution across platforms. Plummer *et al* (173) developed SpatialQM software for imaging platforms to support quality assessment and annotation of cross-platform data. These two studies have laid the foundation for benchmark testing of platform performance required for clinical applications. Nevertheless, multiple rounds of large-scale benchmarking have consistently shown that the standardization process for ST platforms remains constrained by three core challenges. First, there is a lack of quantitative comparability. Platforms exhibit substantial differences in key parameters such as molecular capture efficiency, spatial resolution and downstream analytical capabilities, making direct comparison of gene expression levels across platforms difficult. Second, the reliability of spatial coordinates cannot be compared across platforms. Third, spatial barcode-based technologies suffer from spot-swapping issues, while imaging methods are limited by optical diffraction and image registration errors. Therefore, future standardization efforts urgently need to proceed along three fronts: Establishing cross-platform quantitative reference systems, promoting standardized operating procedures and conducting clinically value-driven multicenter cohort studies to evaluate and continuously calibrate platform outputs. Furthermore, as new technologies continue to emerge, standardized assessments must remain dynamically updated to enable researchers and clinicians to make informed decisions based on the latest evidence (174).

When conducting multicenter cohort studies, cross-cohort validation difficulty represents another core bottleneck for the clinical translation of ST. In addition to differences in platform technologies and batch effects, patient phenotypic heterogeneity and variations in clinical sample processing collectively make direct cross-cohort comparison of gene expression nearly impossible. Even under identical technical conditions, the TME and tissue characteristics across cohorts of patients with the same cancer type remain highly variable, preventing the validation of transferable spatial signatures (175). For testing centers that have not yet established standardized collection protocols for FF/FFPE samples, discrepancies in any step, collection, storage or sectioning, can amplify cross-cohort inconsistency by affecting RNA quality and spatial feature integrity. The breakthrough for achieving cross-cohort validation may lie in establishing standardized quality control metrics applicable to clinical samples, developing more interpretable and robust integration algorithms and, on this basis, conducting large-scale, multicenter prospective cohort studies (173).

Integrating machine learning: A key path to overcoming clinical translation barriers in spatial omics. As a key branch of artificial intelligence, machine learning identifies data patterns through mathematical algorithms to make predictions (176,177) and can efficiently process large datasets while automating decision-making. In recent years, machine learning has been increasingly applied to oncology research. Leveraging advances in omics technologies, multi-level tumor-related data can now be obtained. Large-scale data analysis, while illuminating the path to cancer therapy, requires substantial human effort. The introduction of machine learning offers a new solution for faster and more accurate assessment of immunotherapy efficacy and prognosis in patients with cancer. Trained on large-scale datasets, machine learning algorithms can help improve the accuracy of image segmentation and deconvolution in ST, as well as correct batch effects, positioning them as a powerful tool to overcome clinical translation barriers in ST technology. Furthermore, the deep integration of machine learning with spatial omics has given rise to multimodal data integration and 3D tissue reconstruction, facilitating the construction of human tumor molecular atlases and deepening the understanding of tumor progression.

The iterative evolution of machine learning tools. Machine learning methods are primarily divided into three categories: supervised learning, unsupervised learning and reinforcement learning. In supervised learning, each sample is labeled with an outcome or diagnosis by an expert; these labeled datasets are used to train models by identifying complex patterns within the labeled training data, which can then be applied to make decisions or predictions on new, unseen data. Applications include regression for predicting continuous variables, classification for identifying categories and image segmentation for automatic detection of relevant regions. Unsupervised learning does not rely on labels and aims to discover latent patterns within data, which can be used to identify drug interactions. Reinforcement learning is an autonomous system that learns through trial and error (178-180). Although most machine learning algorithms were developed as early as the 1950s, advances in big data and computational power have driven a profound transformation over the past two decades, evolving the field from task-specific tools to general-purpose, robust and highly transferable foundation models. At the core of this evolution are models such as Nicheformer (181) and Novae (182), which are pre-trained on massive datasets and capable of handling diverse tasks including cell annotation, spatial domain identification and batch correction. Concurrently, model architectures have evolved toward more refined feature learning. Graph contrastive learning approaches such as AugGCL (183) and SpaMGCL have enabled more robust handling of data noise and sparsity. At the application level, collaboration among models has become increasingly close; models such as STransfer (184) and spRefine (185) can efficiently transfer knowledge, considerably reducing manual effort.

In the medical field, machine learning holds substantial promise as an adjunct clinical tool for cancer detection and disease prediction. Deep learning, a subdiscipline of machine

learning, automatically extracts features from low to high dimensions through neural networks trained on large amounts of data, learning complex input-output mappings. Tools in this field have evolved from early proof-of-concept models such as spaGCN and ST-Net, which were used for spatial domain detection and gene imputation but had limited cross-cohort validation and generalizability, to more sophisticated architectures. Subsequent models, including XFuse and DeepSpacE, have introduced probabilistic inference and validation across multiple cancer types, advancing the development of generalizable frameworks (6).

Addressing the limitations of traditional ST technologies. As discussed in previous sections, ST technology still faces numerous challenges in areas such as cell segmentation accuracy, RNA detection efficiency, batch effect removal and modeling of intercellular communication. These technical limitations have, to some extent, hindered the clinical translation of ST. In recent years, machine learning methods, particularly deep learning and graph neural networks, have garnered attention for their powerful feature extraction and pattern recognition capabilities and have been successfully applied to address the aforementioned shortcomings of ST technology.

In the area of cell segmentation and type annotation, traditional methods struggle to distinguish between spatially adjacent cells that are morphologically similar but functionally heterogeneous. To address this, the JSTA framework proposes a computational strategy that jointly performs cell segmentation and type annotation. By incorporating cell type-specific gene expression as prior knowledge, it effectively constrains the consistency between segmentation boundaries and annotation results. Simulation experiments have shown that this approach improves the accuracy of RNA molecule assignment by >45% (158).

In improving deconvolution accuracy, existing methods typically rely on single-cell RNA-seq data to construct reference matrices. However, due to data noise, batch effects and spatial heterogeneity, deconvolution results often contain biases. To overcome these limitations, recent trends have focused on multimodal data fusion. One approach integrates H&E-stained tissue images, extracting cellular morphological features using segmentation algorithms or deep convolutional networks. Another approach integrates spatial coordinate information, employing spatial autocorrelation models or graph neural networks to enhance the spatial smoothness of deconvolution results. Representative tools have demonstrated notable success: Spatial-ID significantly improves cell type mapping accuracy through transfer learning and spatial embedding strategies. STANN uses deep neural networks to achieve cross-modal mapping from single-cell data to ST data. BANKSY combines molecular features of individual cells with information from their local microenvironment, orienting cell phenotype inference around tissue spatial architecture (159). The deep neural network-based spatial cell typing method incorporates an enhanced gene selection strategy and lightweight deep neural network for data training, providing a faster and more accurate solution for ST data analysis, with high accuracy in cell type identification across different brain regions, species and ST platforms (186).

In terms of spatial feature extraction and spatial domain identification, various machine learning models have been integrated into ST analysis pipelines. STLearn provides a deep learning method that extracts tissue section image features as additional model inputs. SpaGCN constructs a graph network based on spatial proximity relationships among target spots and employs a graph convolutional network to learn their spatial distribution features. STAGATE introduces a cell type-aware attention mechanism that expands the structure of the neighborhood graph network to enhance local resolution, with a particular focus on improving boundary detection between distinct spatial domains. GraphST integrates similarity information from gene expression profiles during graph construction as an additional spatial criterion for edge connectivity. SEDR, as the first analytical tool designed for integrated ST datasets, employs a graph autoencoder to represent spatial features while minimizing batch effects induced by multi-sample integration through latent space constraints.

In batch effect removal, the gene spatial integration (GSI) pipeline employs an autoencoder network to extract the native spatial distribution information of gene expression and project it into a common feature space alongside expression features, thereby achieving seamless integration of multiple spatial datasets while preserving biological variation. Application of GSI to the human dorsolateral prefrontal cortex dataset demonstrated that this method stably improves the performance of mainstream clustering tools such as Seurat. Gene spatial distribution, as an independent information dimension, holds significant value in integrative analysis and batch effect removal is necessary for achieving fine-grained tissue feature characterization (163).

In modeling intercellular communication, systematic dissection of L-R interactions depends on experimentally validated L-R databases, yet current resources remain incomplete. Recently, breakthroughs in deep learning-based protein structure prediction tools, such as AlphaFold and related derivatives, have made it possible to predict protein complex structures, particularly high-confidence configurations of L-R complexes, at scale. However, it must be noted that these predictions are computational inferences rather than experimentally validated facts and thus carry inherent uncertainty and risk of false positives. Therefore, careful evaluation of predicted data, clear labeling of computationally inferred results and increased transparency in database construction are key prerequisites for ensuring the scientific and reliable use of L-R datasets now and in the future (165).

In summary, machine learning methods hold potential for addressing the limitations of traditional ST technologies across multiple levels, including cell segmentation, deconvolution, spatial feature extraction, batch effect correction and intercellular communication modeling. With the continued development of new paradigms such as multimodal fusion and self-supervised learning, machine learning is expected to propel ST into a new phase characterized by higher accuracy, enhanced interpretability and improved cross-platform integration capability.

Future prospects of deep integration. This shift has enabled larger-scale data training and more diverse functional annotations. The rapid development of various omics technologies,

including ST, has provided machine learning with massive amounts of high-quality analytical data. The effective integration of the two holds promise for constructing more comprehensive maps of the TME, thereby enabling a more systematic understanding and analysis of tumor progression.

Classical ST studies have revealed spatial features of the TME that limit tumor prognosis. However, due to the limited sample sizes amenable to manual analysis, sequencing results often lack broad representativeness, impeding subsequent translational research. The introduction of machine learning has made large-scale ST data analysis feasible (187) thereby facilitating the construction of high-resolution TME molecular atlases. For example, Roller *et al* (188) developed a gene expression-based precision immunophenotyping tool to reflect the spatial infiltration patterns of CD8+ lymphocytes in the TME based on CD8 immunohistochemistry analysis of 2,023 tumor samples from patients. Similarly, Sun *et al* (189) constructed a neoantigen-reactive T cell atlas from single-cell transcriptomic data of thousands of tumor-infiltrating lymphocytes and built a gene-based machine learning model to accelerate the identification of neoantigen T cell receptors (Neo TCRs) and the engineering of Neo T cells for therapeutic purposes.

Multi-omics joint analysis is increasingly becoming a new trend in tumor immunology research (190-193). Machine learning models, by learning shared representations across different molecular modalities such as transcriptomics, proteomics and metabolomics, can effectively integrate these data while preserving their multi-dimensional spatial information. For example, tools including MUSE, SpatialGlue and MISO employ neural network architectures to align molecular information of varying resolutions, dynamic ranges and biological origins, enabling integrative analysis of multimodal data. Wu *et al* (194) developed an interpretable multimodal deep learning framework based on ST and spatial proteomics inputs, using a graph neural network approach, and achieved excellent performance in predicting immunotherapy response in patients with HCC. Stupichev *et al* (195) adopted an artificial intelligence-based multimodal approach to combine multiple TME-related biomarkers into a composite score for patients with ccRCC who respond favorably to immunotherapy, thereby overcoming the low predictive power of single biomarkers. Even in the face of highly heterogeneous molecular and morphological data, machine learning algorithms can achieve effective integration. He *et al* (196) developed a deep learning algorithm trained on 30,612 spatially resolved gene expression data points matched with histopathological images from 23 patients with breast cancer, enabling direct prediction of spatially resolved transcriptomes from tissue images and offering the possibility of image-based screening for spatial variation in molecular biomarkers. Bell *et al* (197) established a semi-supervised spatial multi-omics integration pipeline combining imaging, spatial ST, and single-cell RNA-seq. By performing ST and single-cell analysis on FFPE samples from pancreatic intraepithelial neoplasia (PanINs), they found that as lesions progress, CAFs transition from an inflammatory to a proliferative signaling state. This analytical framework has broad applicability and can be used to dissect spatiotemporal evolutionary dynamics across multiple cancer types.

In the future, the deep integration of machine learning with spatial omics will further extend into three-dimensional spatial modeling, digital twin construction and spatiotemporal dynamic analysis. Three-dimensional reconstruction can restore the authentic structure of tissues within their native environment. Digital twins integrate multimodal data to build patient-specific virtual tissue models, enabling real-time simulation of disease progression and therapeutic response. Spatiotemporal modeling helps reveal the dynamic principles underlying cell state transitions and microenvironment evolution. The synergistic development of these cutting-edge technologies will drive tumor research from static description toward dynamic prediction, providing a solid theoretical foundation and technical support for precision medicine and early intervention.

5. Outlook

Considerable progress has been made in ST, yet transforming it into a core driving force for tumor immunology research still requires confronting the most pressing unresolved questions in the field and defining clear priorities accordingly. At the level of experimental design, the greatest bottleneck is the 'spatial snapshot' mindset, the vast majority of studies describe static maps at a single time point, failing to distinguish causality from correlation. Therefore, the top priority is to establish standardized time-series spatial sampling models that incorporate key time points including baseline, early treatment response and resistance/relapse in organoids, animal models and clinical specimens, thereby capturing the dynamic evolution of the microenvironment. In terms of computational benchmarking, differences across platforms in resolution, sensitivity and analytical assumptions lead to biological conclusions that are highly dependent on the technological approach. The field critically lacks cross-platform comparable benchmark datasets. There is an urgent need to initiate systematic inter-platform benchmarking studies that apply mainstream technologies in parallel to the same set of tissue samples and make raw data along with standardized analysis pipelines publicly available. At the clinical validation level, although spatial biomarkers are being identified at a rapid pace, the vast majority lack validation in prospective cohorts and cross-platform definition of prognostic thresholds. The core priority is to establish standardized quality control metrics applicable to clinical samples and to launch multicenter prospective clinical trials to evaluate the independent predictive value of spatial parameters compared with conventional biomarkers.

The deep integration of high-resolution ST with spatial proteomics, spatial metabolomics and high-precision imaging technologies holds promise for constructing a multi-dimensional spatiotemporal atlas of the tumor immune ecosystem that encompasses gene expression, protein function, metabolic activity and intercellular interactions. From the perspective of technological development, the core direction of ST lies in the deep fusion of sequencing-based and imaging-based approaches: Sequencing-based methods excel at whole-transcriptome discovery but have limited resolution, whereas imaging-based methods achieve subcellular precision but are constrained by predefined gene panels. Future breakthroughs include the development of spatial multi-omics to enable multimodal detection on the same tissue section, the extension of analysis into three-dimensional space through tissue

clearing technologies, the incorporation of machine learning algorithms and the advancement of standardized workflows compatible with FFPE samples and cross-platform validation. On this basis, future research needs to extend into the temporal dimension, establishing time-series ST atlases that cover the entire process of tumor initiation, progression and treatment, thereby revealing the dynamic evolutionary trajectory of the microenvironment under therapeutic pressure and elucidating the formation and dissolution of immune exclusion barriers, the spatiotemporal sequence of T cell exhaustion and the spatial expansion patterns of drug-resistant clones. Concurrently, the deep integration of multimodal data will establish a complete functional chain from gene expression to protein function to metabolic activity. Combined with three-dimensional imaging technologies, this approach holds promise for constructing a four-dimensional tumor immune ecosystem. Furthermore, structure-based large language models or generative artificial intelligence methods should be developed to predict novel L-R binding pairs directly from protein sequences or spatial structures without relying on existing databases, followed by *in situ* validation incorporating spatial proximity relationships, thereby providing new molecular targets for spatially guided intervention.

Currently, the tension between the highly organized, cancer type-specific nature of microenvironment remodeling mechanisms and cross-cancer universal principles, as well as the gap between physical proximity and actual intercellular interactions, remain core challenges in the field. In the future, integrating technologies such as spatial lineage tracing, *in situ* perturbation and proximity labeling holds promise for transforming these static associations into direct validation of dynamic functional interactions. In summary, ST is driving tumor immunology research from spatial atlas mapping toward mechanistic dissection and clinical translation. By defining three major priorities, experimental design, computational benchmarking and clinical validation, and introducing time-series sampling, multi-omics integration and AI-driven L-R prediction, the field will achieve comprehensive and dynamic dissection of the tumor immune microenvironment, laying a solid foundation for spatially guided precision immunotherapy.

Acknowledgements

Not applicable.

Funding

The present review was supported by National Natural Science Foundation of China (grant no. 82472701).

Availability of data and materials

Not applicable.

Authors' contributions

JJ, XT, YC, QY and BS contributed to writing-original draft, writing-review and editing. JM contributed to writing-review and editing, and funding acquisition. Data authentication not applicable. All authors read and approved the final manuscript.

Ethics approval and consent to participate

Not applicable.

Patient consent for publication

Not applicable.

Competing interests

The authors declare that they have no competing interests.

References

1. Fu T, Dai LJ, Wu SY, Xiao Y, Ma D, Jiang YZ and Shao ZM: Spatial architecture of the immune microenvironment orchestrates tumor immunity and therapeutic response. J Hematol Oncol 14: 98, 2021.
2. Aliazis K, Christofides A, Shah R, Yeo YY, Jiang S, Charest A and Boussiotis VA: The tumor Microenvironment's role in the response to immune checkpoint blockade. Nat Cancer 6: 924-937, 2025.
3. Chen MM, Gao Q, Ning H, Chen K, Gao Y, Yu M, Liu CQ, Zhou W, Pan J, Wei L, *et al*: Integrated single-cell and spatial transcriptomics uncover distinct cellular subtypes involved in neural invasion in pancreatic cancer. Cancer Cell 43: 1656-1676. e10, 2025.
4. Lin Z, Zhou Y, Liu Z, Nie W, Cao H, Li S, Li X, Zhu L, Lin G, Ding Y, *et al*: Deciphering the tumor immune microenvironment: Single-cell and spatial transcriptomic insights into cervical cancer fibroblasts. J Exp Clin Cancer Res 44: 194, 2025
5. Liu Y, Dai Y and Wang L: Spatial omics at the forefront: Emerging technologies, analytical innovations, and clinical applications. Cancer Cell 44: 24-49, 2026.
6. Lazar E and Lundeberg J: Spatial architecture of development and disease. Nat Rev Genet 27: 118-136, 2026.
7. Arora R, Cao C, Kumar M, Sinha S, Chanda A, McNeil R, Samuel D, Arora RK, Matthews TW, Chandarana S, *et al*: Spatial transcriptomics reveals distinct and conserved tumor core and edge architectures that predict survival and targeted therapy response. Nat Commun 14: 5029, 2023.
8. Zhou T, Wu Y, Li S, Qiu X, Liu E, Xie Z, Shi X, Zhang Y, Ma G, Guo W, *et al*: Multi-omic analysis of gallbladder cancer identifies distinct tumor microenvironments associated with disease progression. Nat Genet 57: 1935-1949, 2025.
9. Perez-Villatoro F, Shabanova A, van Wagensveld L, Junquera A, Niemiec I, Hincapie-Otero MM, Kang Z, Falco MM, Birgin K, Wolf S, *et al*: Single-cell spatial atlas of High-grade serous ovarian cancer uncovers MHC Class II as a key predictor of spatial tumor ecosystems and clinical outcomes. Cancer Discov 16: 1100-1125, 2026.
10. Wang X, Wang Z, Liao Q, Yuan P, Mei J, Zhang Y, Wu C, Kang X, Zheng S, Yang C, *et al*: Spatially resolved atlas of breast cancer uncovers intercellular machinery of venular niche governing lymphocyte extravasation. Nat Commun 16: 3348, 2025.
11. Dong H, Wang X, Zheng Y, Li J, Liu Z, Wang A, Shen Y, Wu D and Cui H: Mapping the rapid growth of multi-omics in tumor immunotherapy: Bibliometric evidence of technology convergence and paradigm shifts. Hum Vaccin Immunother 21: 2493539, 2025.
12. Buenrostro JD, Giresi PG, Zaba LC, Chang HY and Greenleaf WJ: Transposition of native chromatin for fast and sensitive epigenomic profiling of open chromatin, DNA-binding proteins and nucleosome position. Nat Methods 10: 1213-1218, 2013.
13. Dey SS, Kester L, Spanjaard B, Bienko M and van Oudenaarden A: Integrated genome and transcriptome sequencing of the same cell. Nat Biotechnol 33: 285-289, 2015.
14. Guo H, Zhu P, Wu X, Li X, Wen L and Tang F: Single-cell methylome landscapes of mouse embryonic stem cells and early embryos analyzed using reduced representation bisulfite sequencing. Genome Res 23: 2126-2135, 2013.
15. Nagano T, Lubling Y, Stevens TJ, Schoenfelder S, Yaffe E, Dean W, Laue ED, Tanay A and Fraser P: Single-cell Hi-C reveals cell-to-cell variability in chromosome structure. Nature 502: 59-64, 2013.

16. Macaulay IC, Haerty W, Kumar P, Li YI, Hu TX, Teng MJ, Goolam M, Saurat N, Coupland P, Shirley LM, *et al*: G&T-seq: Parallel sequencing of single-cell genomes and transcriptomes. Nat Methods 12: 519-522, 2015.
17. Heumos L, Schaar AC, Lance C, Litinetskaya A, Drost F, Zappia L, Lucken MD, Strobl DC, Henao J, Curion F, *et al*: Best practices for single-cell analysis across modalities. Nat Rev Genet 24: 550-572, 2023.
18. He J, Deng C, Krall L and Shan Z: ScRNA-seq and ST-seq in liver research. Cell Regen 12: 11, 2023.
19. Stahl PL, Salmen F, Vickovic S, Lundmark A, Navarro JF, Magnusson J, Giacomello S, Asp M, Westholm JO, Huss M, *et al*: Visualization and analysis of gene expression in tissue sections by spatial transcriptomics. Science 353: 78-82, 2016.
20. Maynard KR, Collado-Torres L, Weber LM, Uytingco C, Barry BK, Williams SR, Catallini JL II, Tran MN, Besich Z, Tippani M, *et al*: Transcriptome-scale spatial gene expression in the human dorsolateral prefrontal cortex. Nat Neurosci 24: 425-436, 2021.
21. Rodriques SG, Stickels RR, Goeva A, Martin CA, Murray E, Vanderburg CR, Welch J, Chen LM, Chen F and Macosko EZ: Slide-seq: A scalable technology for measuring genome-wide expression at high spatial resolution. Science 363: 1463-1467, 2019.
22. White E and White D: Bibliography of biomedical ultrasound. No. 61. Ultrasound Med Biol 13: 35-50, 1987.
23. Ke R, Mignardi M, Pacureanu A, Svedlund J, Botling J, Wahlby C and Nilsson M: In situ sequencing for RNA analysis in preserved tissue and cells. Nat Methods 10: 857-860, 2013.
24. Darmanis S, Sloan SA, Croote D, Mignardi M, Chernikova S, Samghababi P, Zhang Y, Neff N, Kowarsky M, Caneda C, *et al*: Single-cell RNA-Seq analysis of infiltrating neoplastic cells at the migrating front of human Glioblastoma. Cell Rep 21: 1399-1410, 2017.
25. Carow B, Hauling T, Qian X, Kramnik I, Nilsson M and Rottenberg ME: Spatial and temporal localization of immune transcripts defines hallmarks and diversity in the tuberculosis granuloma. Nat Commun 10: 1823, 2019.
26. Tiklova K, Bjorklund AK, Lahti L, Fiorenzano A, Nolbrant S, Gillberg L, Volakakis N, Yokota C, Hilscher MM, Hauling T, *et al*: Single-cell RNA sequencing reveals midbrain dopamine neuron diversity emerging during mouse brain development. Nat Commun 10: 581, 2019.
27. Chen KH, Boettiger AN, Moffitt JR, Wang S and Zhuang X: RNA imaging. Spatially resolved, highly multiplexed RNA profiling in single cells. Science 348: aaa6090, 2015.
28. Eng CL, Lawson M, Zhu Q, Dries R, Koulena N, Takei Y, Yun J, Cronin C, Karp C, Yuan GC and Cai L: Transcriptome-scale super-resolved imaging in tissues by RNA seqFISH. Nature 568: 235-239, 2019.
29. Moffitt JR, Hao J, Wang G, Chen KH, Babcock HP and Zhuang X: High-throughput single-cell gene-expression profiling with multiplexed error-robust fluorescence in situ hybridization. Proc Natl Acad Sci USA 113: 11046-11051, 2016.
30. Wang G, Moffitt JR and Zhuang X: Multiplexed imaging of high-density libraries of RNAs with MERFISH and expansion microscopy. Sci Rep 8: 4847, 2018.
31. Lubeck E, Coskun AF, Zhiyentayev T, Ahmad M and Cai L: Single-cell in situ RNA profiling by sequential hybridization. Nat Methods 11: 360-361, 2014.
32. Shah S, Lubeck E, Zhou W and Cai L: In situ transcription profiling of single cells reveals spatial organization of cells in the mouse hippocampus. Neuron 92: 342-357, 2016.
33. Xia C, Babcock HP, Moffitt JR and Zhuang X: Multiplexed detection of RNA using MERFISH and branched DNA amplification. Sci Rep 9: 7721, 2019.
34. Dodt HU, Leischner U, Schierloh A, Jahrling N, Mauch CP, Deininger K, Deussing JM, Eder M, Zieglgansberger W and Becker K: Ultramicroscopy: Three-dimensional visualization of neuronal networks in the whole mouse brain. Nat Methods 4: 331-336, 2007.
35. Erturk A, Becker K, Jahrling N, Mauch CP, Hojer CD, Egen JG, Hellal F, Bradke F, Sheng M and Dodt HU: Three-dimensional imaging of solvent-cleared organs using 3DISCO. Nat Protoc 7: 1983-995, 2012.
36. Renier N, Wu Z, Simon DJ, Yang J, Ariel P and Tessier-Lavigne M: iDISCO: A simple, rapid method to immunolabel large tissue samples for volume imaging. Cell 159: 896-910, 2014.
37. Hou B, Zhang D, Zhao S, Wei M, Yang Z, Wang S, Wang J, Zhang X, Liu B, Fan L, *et al*: Scalable and DiI-compatible optical clearance of the mammalian brain. Front Neuroanat 9: 19, 2015.
38. Hama H, Kurokawa H, Kawano H, Ando R, Shimogori T, Noda H, Fukami K, Sakaue-Sawano A and Miyawaki A: Scale: A chemical approach for fluorescence imaging and reconstruction of transparent mouse brain. Nat Neurosci 14: 1481-1488, 2011.
39. Ke MT, Fujimoto S and Imai T: SeeDB: A simple and morphology-preserving optical clearing agent for neuronal circuit reconstruction. Nat Neurosci 16: 1154-1161, 2013.
40. Susaki EA, Tainaka K, Perrin D, Kishino F, Tawara T, Watanabe TM, Yokoyama C, Onoe H, Eguchi M, Yamaguchi S, *et al*: Whole-brain imaging with single-cell resolution using chemical cocktails and computational analysis. Cell 157: 726-739, 2014.
41. Tomer R, Ye L, Hsueh B and Deisseroth K: Advanced CLARITY for rapid and high-resolution imaging of intact tissues. Nat Protoc 9: 1682-1697, 2014.
42. Murray E, Cho JH, Goodwin D, Ku T, Swaney J, Kim SY, Choi H, Park YG, Park JY, Hubbert A, *et al*: Simple, scalable proteomic imaging for high-dimensional profiling of intact systems. Cell 163: 1500-1514, 2015.
43. Lee E and Sun W: ACT-PRESTO: Biological tissue clearing and immunolabeling methods for volume imaging. J Vis Exp: 54904, 2016 doi: 10.3791/54904.
44. Park YG, Sohn CH, Chen R, McCue M, Yun DH, Drummond GT, Ku T, Evans NB, Oak HC, Trieu W, *et al*: Protection of tissue physicochemical properties using polyfunctional crosslinkers. Nat Biotechnol: Dec 17, 2018 (Epub ahead of print). doi:10.1038/nbt.4281.
45. Guo P and Deng Y: Spatial Omics: Navigating neuroscience research into the new era. Adv Neurobiol 41: 133-149, 2024.
46. Jonstrup SP, Koch J and Kjems J: A microRNA detection system based on padlock probes and rolling circle amplification. RNA 12: 1747-1752, 2006.
47. Krzywkowski T, Hauling T and Nilsson M: In situ single-molecule RNA genotyping using padlock probes and rolling circle amplification. Methods Mol Biol 1492: 59-76, 2017.
48. Yan G, Hua SH and Li JJ: Categorization of 34 computational methods to detect spatially variable genes from spatially resolved transcriptomics data. Nat Commun 16: 1141, 2025.
49. Choi J, Li J, Ferdous S, Liang Q, Moffitt JR and Chen R: Spatial organization of the mouse retina at single cell resolution by MERFISH. Nat Commun 14: 4929, 2023.
50. Xia C, Fan J, Emanuel G, Hao J and Zhuang X: Spatial transcriptome profiling by MERFISH reveals subcellular RNA compartmentalization and cell cycle-dependent gene expression. Proc Natl Acad Sci USA 116: 19490-19499, 2019.
51. Weber C, Defard T, Sturmach C, Lelek M, Laporte H, Mallick A, Gariboldi MI, Londono-Vallejo JA, Walter T, Fouillade C, *et al*: autoFISH: A modular toolbox for sequential single-molecule RNA FISH experiments. Commun Biol 9: 752, 2026.
52. Haimovich G and Gerst JE: Single-molecule fluorescence in situ hybridization (smFISH) for RNA detection in adherent animal cells. Bio Protoc 8: e3070, 2018.
53. Lee H, Marco Salas S, Gyllborg D and Nilsson M: Direct RNA targeted in situ sequencing for transcriptomic profiling in tissue. Sci Rep 12: 7976, 2022.
54. Lemes CC, Germano da Silva A, Ribeiro DA and Malinverni ACM: Challenges and solutions in FISH for formalin-fixed paraffin-embedded tissue: A scoping review. Microsc Res Tech 88: 270-278, 2025.
55. Alon S, Goodwin DR, Sinha A, Wassie AT, Chen F, Daugharthy ER, Bando Y, Kajita A, Xue AG, Marrett K, *et al*: Expansion sequencing: Spatially precise in situ transcriptomics in intact biological systems. Science 371: eaax2656, 2021.
56. Bostrom J, Zapała M and Adameyko I: Boosting multiplexing capabilities for error-robust spatial transcriptomic methods using a set exchange approach. Sci Adv 11: eadr4026, 2025.
57. Gyllborg D, Langseth CM, Qian X, Choi E, Salas SM, Hilscher MM, Lein ES and Nilsson M: Hybridization-based in situ sequencing (HybISS) for spatially resolved transcriptomics in human and mouse brain tissue. Nucleic Acids Res 48: e112, 2020.
58. Wagner J, Rapsomaniki MA, Chevrier S, Anzeneder T, Langwieder C, Dykgers A, Rees M, Ramaswamy A, Muenst S, Soysal SD, *et al*: A single-cell atlas of the tumor and immune ecosystem of human breast cancer. Cell 177: 1330-1345.e18, 2019.
59. Kleshchevnikov V, Shmatko A, Dann E, Aivazidis A, King HW, Li T, Elmentaite R, Lomakin A, Kedlian V, Gayoso A, *et al*: Cell2location maps fine-grained cell types in spatial transcriptomics. Nat Biotechnol 40: 661-671, 2022.
60. Elosua-Bayes M, Nieto P, Mereu E, Gut I and Heyn H: SPOTlight: Seeded NMF regression to deconvolute spatial transcriptomics spots with single-cell transcriptomes. Nucleic Acids Res 49: e50, 2021.

61. Biancalani T, Scalia G, Buffoni L, Avasthi R, Lu Z, Sanger A, Tokcan N, Vanderburg CR, Segerstolpe A, Zhang M, *et al*: Deep learning and alignment of spatially resolved single-cell transcriptomes with Tangram. Nat Methods 18: 1352-1362, 2021.
62. Toninelli M, Rossetti G and Pagani M: Charting the tumor microenvironment with spatial profiling technologies. Trends Cancer 9: 1085-1096, 2023.
63. Xie Z, Li X and Mora A: A comparison of cell-cell interaction prediction tools based on scRNA-seq data. Biomolecules 13: 1211, 2023.
64. Guan P, Cai W, Wu K, Jiang F, Wu J, Zhai X and Zeng M: Intercellular communication-related molecular subtypes and a gene signature identified by the single-cell RNA sequencing combined with a transcriptomic analysis. Dis Markers 2022: 6837849, 2022.
65. Matsui I, Matsumoto A, Inoue K, Katsuma Y, Yasuda S, Shimada K, Sakaguchi Y, Mizui M, Kaimori JY, Takabatake Y and Isaka Y: Single cell RNA sequencing uncovers cellular developmental sequences and novel potential intercellular communications in embryonic kidney. Sci Rep 11: 73, 2021.
66. Noel F, Massenet-Regad L, Carmi-Levy I, Cappuccio A, Grandclaudon M, Trichot C, Kieffer Y, Mechta-Grigoriou F and Soumelis V: Dissection of intercellular communication using the transcriptome-based framework ICELLNET. Nat Commun 12: 1089, 2021.
67. Pelka K, Hofree M, Chen JH, Sarkizova S, Pirl JD, Jorgji V, Bejnood A, Dionne D, Ge WH, Xu KH, *et al*: Spatially organized multicellular immune hubs in human colorectal cancer. Cell 184: 4734-4752.e20, 2021.
68. Yang CC, Lin CY, Yuan HY, Huang HC and Juan HF: Mass spectrometry-based human spatial omics: Fundamentals, innovations, and applications. J Biomed Sci 33: 16, 2026.
69. See JE, Barlow S, Arjumand W, DuBose H, Segato Dezem F and Plummer J: Spatial omics: Applications and utility in profiling the tumor microenvironment. Cancer Metastasis Rev 44: 87, 2025.
70. Wu X, Xu W, Lin D, Sun L, Loo LH, Dai J and Cao G: The application and prospects of spatial omics technologies in clinical medical research and molecular diagnostics. J Genet Genomics 53: 181-196, 2026.
71. Ji L: Spatial multi-omics technologies and applications in cancer. Biosystems 257: 105576, 2025.
72. Hsieh WC, Budiarto BR, Wang YF, Lin CY, Gwo MC, So DK, Tzeng YS and Chen SY: Spatial multi-omics analyses of the tumor immune microenvironment. J Biomed Sci 29: 96, 2022.
73. Chu X, Tian Y and Lv C: Decoding the spatiotemporal heterogeneity of tumor-associated macrophages. Mol Cancer 23: 150, 2024.
74. Chang J, Lu J, Liu Q, Xiang T, Zhang S, Yi Y, Li D, Liu T, Liu Z, Chen X, *et al*: Single-cell multi-stage spatial evolutional map of esophageal carcinogenesis. Cancer Cell 43: 380-397.e7, 2025.
75. Peng F, Sinjab A, Dai Y, Treekitkarnmongkol W, Yang S, Gomez Bolanos LI, Zhou T, Chen M, Serrano AG, Krishna A, *et al*: Multimodal spatial-omics reveal co-evolution of alveolar progenitors and proinflammatory niches in progression of lung precursor lesions. Cancer Cell 44: 321-339.e13, 2026.
76. Reyes J, Del Priore I, Chaikovsky AC, Pasnuri N, Elhossiny AM, Park J, Weiler P, Krause T, Moorman A, Snopkowski C, *et al*: Oncogenic and tumor-suppressive forces converge on a progenitor niche at the benign-to-malignant transition. Cell 189: 2875-2897.e53, 2026.
77. Cardoso EC, Lee H, England FJ, Cho H, Lu R, Varankar SS, Park MS, Rekhtman N, Koo BK, Simons BD, *et al*: Early fibrotic niches establish tumour-permissive microenvironments. Nature 653: 254-264, 2026.
78. Zhang G, Zhang X, Pan W, Chen X, Wan L, Liu C, Yong Y, Zhao Y, Sang S, Zhang L, *et al*: Dissecting the spatial and single-cell transcriptomic architecture of cancer stem cell niche driving tumor progression in gastric cancer. Adv Sci (Weinh) 12: e2413019, 2025.
79. Gao P, Zuo C, Yuan W, Cai J, Chai X, Gong R, Yu J, Yao L, Su W, Liu Z, *et al*: Spatiotemporal multi-omics analysis uncovers NAD-dependent immunosuppressive niche triggering early gastric cancer. Signal Transduct Target Ther 10: 313, 2025.
80. Ma L, Xiong B, Liu M and Tan K: Cellular neighborhoods in cancer. Nat Cancer 7: 16-28, 2026.
81. de Visser KE and Joyce JA: The evolving tumor microenvironment: From cancer initiation to metastatic outgrowth. Cancer Cell 41: 374-403, 2023.
82. Oliveira MF, Romero JP, Chung M, Williams SR, Gottscho AD, Gupta A, Pilipauskas SE, Mohabbat S, Raman N, Sukovich DJ, *et al*: High-definition spatial transcriptomic profiling of immune cell populations in colorectal cancer. Nat Genet 57: 1512-1523, 2025.
83. Fridman WH, Meylan M, Petitprez F, Sun CM, Italiano A and Sautes-Fridman C: B cells and tertiary lymphoid structures as determinants of tumour immune contexture and clinical outcome. Nat Rev Clin Oncol 19: 441-457, 2022.
84. Cho KS, Liu Y, Pei G, Chen J, Dai Y, Liu Y, Zhou T, Bougouin A, Serrano A, Wani K, *et al*: Pan-cancer spatial atlas of tertiary lymphoid structures. Science 392: eadz2742, 2026.
85. Wang Z, Ge Q, Mo R, Lu J, Tian X, Anwaier A, Ye S, Zhou S, Guo W, Cai C, *et al*: Spatial and maturity heterogeneity of tertiary lymphoid structures shapes immune microenvironment and progression in prostate cancer. J Natl Cancer Cent 5: 501-514, 2025.
86. Tang Z, Bai Y, Fang Q, Yuan Y, Zeng Q, Chen S, Xu T, Chen J, Tan L, Wang C, *et al*: Spatial transcriptomics reveals tryptophan metabolism restricting maturation of intratumoral tertiary lymphoid structures. Cancer Cell 43: 1025-1044.e14, 2025.
87. Meylan M, Petitprez F, Becht E, Bougouin A, Pupier G, Calvez A, Giglioli I, Verkarre V, Lacroix G, Verneau J, *et al*: Tertiary lymphoid structures generate and propagate anti-tumor antibody-producing plasma cells in renal cell cancer. Immunity 55: 527-541.e5, 2022.
88. Liu Y, Ye SY, He S, Chi DM, Wang XZ, Wen YF, Ma D, Nie RC, Xiang P, Zhou Y, *et al*: Single-cell and spatial transcriptome analyses reveal tertiary lymphoid structures linked to tumour progression and immunotherapy response in nasopharyngeal carcinoma. Nat Commun 15: 7713, 2024.
89. Zhang Y, Liu G, Zeng Q, Wu W, Lei K, Zhang C, Tang M, Zhang Y, Xiang X, Tan L, *et al*: CCL19-producing fibroblasts promote tertiary lymphoid structure formation enhancing anti-tumor IgG response in colorectal cancer liver metastasis. Cancer Cell 42: 1370-1385.e9, 2024.
90. Xu AM, Haro M, Walts AE, Hu Y, John J, Karlan BY, Merchant A and Orsulic S: Spatiotemporal architecture of immune cells and cancer-associated fibroblasts in high-grade serous ovarian carcinoma. Sci Adv 10: eadk8805, 2024.
91. Zhou S, Ye S, Chen L, Ge Q, Lu J, Anwaier A, Tian X, Wang Z, Zhu S, Chang K, *et al*: Interferon regulatory factor 4 recruits immature b cells to signal tertiary lymphoid structure immaturity and progression of clear cell renal cell carcinoma. Int J Biol Sci 21: 3827-3851, 2025.
92. Liu Y, Dong G, Yu J and Liang P: Integration of single-cell and spatial transcriptomics reveals fibroblast subtypes in hepatocellular carcinoma: Spatial distribution, differentiation trajectories, and therapeutic potential. J Transl Med 23: 198, 2025.
93. Pei G, Min J, Rajapakshe KI, Branchi V, Liu Y, Selvanesan BC, Thege F, Sadeghian D, Zhang D, Cho KS, *et al*: Spatial mapping of transcriptomic plasticity in metastatic pancreatic cancer. Nature 642: 212-221, 2025.
94. Liu Z, Zhang Z, Zhang Y, Zhou W, Zhang X, Peng C, Ji T, Zou X, Zhang Z and Ren Z: Spatial transcriptomics reveals that metabolic characteristics define the tumor immunosuppression microenvironment via iCAF transformation in oral squamous cell carcinoma. Int J Oral Sci 16: 9, 2024.
95. Li C, Guo H, Zhai P, Yan M, Liu C, Wang X, Shi C, Li J, Tong T, Zhang Z, *et al*: Spatial and single-cell transcriptomics reveal a cancer-associated fibroblast subset in HNSCC that restricts infiltration and antitumor activity of CD8+ T cells. Cancer Res 84: 258-275, 2024.
96. Jain S, Rick JW, Joshi RS, Beniwal A, Spatz J, Gill S, Chang AC, Choudhary N, Nguyen AT, Sudhir S, *et al*: Single-cell RNA sequencing and spatial transcriptomics reveal cancer-associated fibroblasts in glioblastoma with protumoral effects. J Clin Invest 133: e147087, 2023.
97. Zhao Z, Cai H, Nie W, Wang X, Zhao Z, Zhao F, Chen Y, Luo Z, Lin Z, Lin L and Ding Y: Ectopic expression of GDF15 in cancer-associated fibroblasts enhances melanoma immunosuppression via the GFRAL/RET cascade. J Immunother Cancer 13: e011036, 2025.
98. Cui X, Liu S, Song H, Xu J and Sun Y: Single-cell and spatial transcriptomic analyses revealing tumor microenvironment remodeling after neoadjuvant chemoimmunotherapy in non-small cell lung cancer. Mol Cancer 24: 111, 2025.
99. Ou Z, Lin S, Qiu J, Ding W, Ren P, Chen D, Wang J, Tong Y, Wu D, Chen A, *et al*: Single-nucleus RNA sequencing and spatial transcriptomics reveal the immunological microenvironment of cervical squamous cell carcinoma. Adv Sci (Weinh) 9: e2203040, 2022.

100. Heming M, Haessner S, Wolbert J, Lu IN, Li X, Brokinkel B, Muther M, Holling M, Stummer W, Thomas C, *et al*: Intratumor heterogeneity and T cell exhaustion in primary CNS lymphoma. Genome Med 14: 109, 2022.
101. Murai H, Kodama T, Maesaka K, Tange S, Motooka D, Suzuki Y, Shigematsu Y, Inamura K, Mise Y, Saiura A, *et al*: Multiomics identifies the link between intratumor steatosis and the exhausted tumor immune microenvironment in hepatocellular carcinoma. Hepatology 77: 77-91, 2023.
102. Li R, Ferdinand JR, Loudon KW, Bowyer GS, Laidlaw S, Muyas F, Mamanova L, Neves JB, Bolt L, Fasouli ES, *et al*: Mapping single-cell transcriptomes in the intra-tumoral and associated territories of kidney cancer. Cancer Cell 40: 1583-1599.e10, 2022.
103. Tietscher S, Wagner J, Anzeneder T, Langwieder C, Rees M, Sobottka B, de Souza N and Bodenmiller B: A comprehensive single-cell map of T cell exhaustion-associated immune environments in human breast cancer. Nat Commun 14: 98, 2023.
104. Xun Z, Zhou H, Shen M, Liu Y, Sun C, Du Y, Jiang Z, Yang L, Zhang Q, Lin C, *et al*: Identification of Hypoxia-ALCAM(high) macrophage-exhausted T cell axis in tumor microenvironment remodeling for immunotherapy resistance. Adv Sci (Weinh) 11: e2309885, 2024.
105. Launonen IM, Niemiec I, Hincapie-Otero M, Erkan EP, Junquera A, Afenteva D, Falco MM, Liang Z, Salko M, Chamchougia F, *et al*: Chemotherapy induces myeloid-driven spatially confined T cell exhaustion in ovarian cancer. Cancer Cell 42: 2045-2063.e10, 2024.
106. Greenwald AC, Darnell NG, Hoefflin R, Simkin D, Mount CW, Gonzalez Castro LN, Harnik Y, Dumont S, Hirsch D, Nomura M, *et al*: Integrative spatial analysis reveals a multi-layered organization of glioblastoma. Cell 187: 2485-2501.e26, 2024.
107. Du Y, Shi J, Wang J, Xun Z, Yu Z, Sun H, Bao R, Zheng J, Li Z and Ye Y: Integration of pan-cancer single-cell and spatial transcriptomics reveals stromal cell features and therapeutic targets in tumor microenvironment. Cancer Res 84: 192-210, 2024.
108. Yeh CY, Aguirre K, Laveroni O, Kim S, Wang A, Liang B, Zhang X, Han LM, Valbuena R, Bassik MC, *et al*: Mapping spatial organization and genetic cell-state regulators to target immune evasion in ovarian cancer. Nat Immunol 25: 1943-1958, 2024.
109. Wang XQ, Danenberg E, Huang CS, Egle D, Callari M, Bermejo B, Dugo M, Zamagni C, Thill M, Anton A, *et al*: Spatial predictors of immunotherapy response in triple-negative breast cancer. Nature 621: 868-876, 2023.
110. Wang Z, Kim SY, Tu W, Kim J, Xu A, Yang YM, Matsuda M, Reolizo L, Tsuchiya T, Billet S, *et al*: Extracellular vesicles in fatty liver promote a metastatic tumor microenvironment. Cell Metab 35: 1209-1226.e13, 2023.
111. Grant G and Ferrer CM: The role of the immune tumor microenvironment in shaping metastatic dissemination, dormancy, and outgrowth. Trends Cell Biol 36: 377-391, 2026.
112. Jimenez-Castano R, Narwade N, Moreno-Bueno G, Sanchez-Laorden B, Galceran J, Youssef KK and Nieto MA: A hormetic transcriptional program coregulates invasion, proliferation and dormancy to define metastatic potential. Nat Commun 17: 3425, 2026.
113. Kan JY, Lee HC, Hou MF, Tsai HP, Jian SF, Chang CY, Tsai PH, Lin YS, Tsai YM, Wu KL, *et al*: Metabolic shifts in lipid utilization and reciprocal interactions within the lung metastatic niche of triple-negative breast cancer revealed by spatial multi-omics. Cell Death Dis 15: 899, 2024.
114. Zuyin L, Zhao L, Qian C, Changkun Z, Delin M, Jialing H, Zhuomiaoyu C, Yuzi L, Jiaxi Z, Jie G and Jiye Z: Single-cell and spatial transcriptomics delineate the microstructure and immune landscape of intrahepatic cholangiocarcinoma in the leading-edge area. Adv Sci (Weinh) 12: e2412740, 2025.
115. Khaliq AM, Rajamohan M, Saeed O, Mansouri K, Adil A, Zhang C, Turk A, Carstens JL, House M, Hayat S, *et al*: Spatial transcriptomic analysis of primary and metastatic pancreatic cancers highlights tumor microenvironmental heterogeneity. Nat Genet 56: 2455-2465, 2024.
116. Haist M, Baertsch MA, Reticker-Flynn NE, Lu G, Kempchen TN, Chu P, Vazquez G, Chen H, Sunwoo JB, Zhang W, *et al*: Lymph node colonization induces tissue remodeling via immunosuppressive fibroblast-myeloid cell niches supporting metastatic tolerance. Cancer Cell 44: 604-623.e9, 2026.
117. Zhang Z, Wu D, Chen R, Zhai M, Yang F, Wang J, Guo L, Liu L, Ying J, Yang L and Zhou M: Single-cell spatial transcriptomics reveals tumor microenvironment heterogeneity in primary and lymph node-metastatic small cell lung cancer. Cell Rep Med 7: 102713, 2026.
118. Wu L, Yan J, Bai Y, Chen F, Zou X, Xu J, Huang A, Hou L, Zhong Y, Jing Z, *et al*: An invasive zone in human liver cancer identified by Stereo-seq promotes hepatocyte-tumor cell crosstalk, local immunosuppression and tumor progression. Cell Res 33: 585-603, 2023.
119. Ma H, Srivastava S, Ho SWT, Xu C, Lian BSX, Ong X, Tay ST, Sheng T, Lum HYJ, Abdul Ghani SAB, *et al*: Spatially resolved tumor ecosystems and cell states in gastric adenocarcinoma progression and evolution. Cancer Discov 15: 767-792, 2025.
120. Chitra U, Arnold BJ, Sarkar H, Sanno K, Ma C, Lopez-Darwin S and Raphael BJ: Mapping the topography of spatial gene expression with interpretable deep learning. Nat Methods 22: 298-309, 2025.
121. Yang S, Zhang D, Sun Q, Nie H, Zhang Y, Wang X, Huang Y and Sun Y: Single-cell and spatial transcriptome profiling identifies the transcription factor BHLHE40 as a driver of EMT in metastatic colorectal cancer. Cancer Res 84: 2202-2217, 2024.
122. Lu Y, Chen Y, Wang Z, Shen H, Xu L, Huang C, Tong Y, Shao Y, Zhang H and Fu Z: Single-cell and spatial transcriptome profiling reveal CTHRC1+ fibroblasts promote EMT through WNT5A signaling in colorectal cancer. J Transl Med 23: 282, 2025.
123. Liu H, Gao J, Feng M, Cheng J, Tang Y, Cao Q, Zhao Z, Meng Z, Zhang J, Zhang G, *et al*: Integrative molecular and spatial analysis reveals evolutionary dynamics and tumor-immune interplay of in situ and invasive acral melanoma. Cancer Cell 42: 1067-1085.e11, 2024.
124. Yang G, Cheng J, Xu J, Shen C, Lu X, He C, Huang J, He M, Cheng J and Wang H: Metabolic heterogeneity in clear cell renal cell carcinoma revealed by single-cell RNA sequencing and spatial transcriptomics. J Transl Med 22: 210, 2024.
125. Chauvin M, Tromelin E, Roche-Prellezo J, Lancia HH, Meinsohn MC, Coletti C, Nguyen NMP, Lafont V, Michaud HA, Mishra R, *et al*: FSTL3 is a biomarker of poor prognosis and associated with immunotherapy resistance in ovarian cancer. J Exp Clin Cancer Res 44: 271, 2025.
126. Luo XR, Huang LZ, Yin J, Xiong ZM, Li WX, Liao C, Lin ML, Huang W and Zhang S: FSTL3 promotes colorectal cancer by activating the HIF1 pathway. Gene 954: 149435, 2025.
127. Meng X, Zhao X, Zhou B, Song W, Liang Y, Liang M, Du M, Shi J and Gao Y: FSTL3 is associated with prognosis and immune cell infiltration in lung adenocarcinoma. J Cancer Res Clin Oncol 150: 17, 2024.
128. Liu YJ, Li JP, Zhang Y, Nie MJ, Zhang YH, Liu SL and Zou X: FSTL3 is a prognostic biomarker in gastric cancer and is correlated with M2 macrophage infiltration. Onco Targets Ther 14: 4099-4117, 2021.
129. Yan J, Wang J, Miao M and Shao Y: Comprehensive pan-cancer analysis indicates key gene of p53-independent apoptosis is a novel biomarker for clinical application and chemotherapy in colorectal cancer. Front Immunol 16: 1571137, 2025.
130. Wang H, Li F, Wang Q, Guo X, Chen X, Zou X and Yuan J: Identifying ADME-related gene signature for immune landscape and prognosis in KIRC by single-cell and spatial transcriptome analysis. Sci Rep 15: 1294, 2025.
131. Zhang S, Yuan L, Danilova L, Mo G, Zhu Q, Deshpande A, Bell ATF, Elisseeff J, Popel AS, Anders RA, *et al*: Spatial transcriptomics analysis of neoadjuvant cabozantinib and nivolumab in advanced hepatocellular carcinoma identifies independent mechanisms of resistance and recurrence. Genome Med 15: 72, 2023.
132. Qin Z, Huang G, Xu J, Pan L, Lan C, Yang Y, Yin Y and Qin Y: Multidimensional transcriptomics based to illuminate the mechanisms of taurine metabolism in immune resistance of pancreatic cancer. Front Immunol 16: 1567805, 2025.
133. Song X, Xiong A, Wu F, Li X, Wang J, Jiang T, Chen P, Zhang X, Zhao Z, Liu H, *et al*: Spatial multi-omics revealed the impact of tumor ecosystem heterogeneity on immunotherapy efficacy in patients with advanced non-small cell lung cancer treated with bispecific antibody. J Immunother Cancer 11: e006234, 2023.
134. Mao Z, Gao Z, Long R, Guo H, Chen L, Huan S and Yin G: Mitotic catastrophe heterogeneity: Implications for prognosis and immunotherapy in hepatocellular carcinoma. Front Immunol 15: 1409448, 2024.

135. Guo J, Tang B, Fu J, Zhu X, Xie W, Wang N, Ding Z, Song Z, Yang Y, Xu G and Xiao X: High-plex spatial transcriptomic profiling reveals distinct immune components and the HLA class I/DNMT3A/CD8 modulatory axis in mismatch repair-deficient endometrial cancer. Cell Oncol (Dordr) 47: 573-585, 2024.
136. Oyoshi H, Du J, Sakai SA, Yamashita R, Okumura M, Motegi A, Hojo H, Nakamura M, Hirata H, Sunakawa H, *et al*: Comprehensive single-cell analysis demonstrates radiotherapy-induced infiltration of macrophages expressing immunosuppressive genes into tumor in esophageal squamous cell carcinoma. Sci Adv 9: eadh9069, 2023.
137. Mendoza-Valderrey A, Choe J, Kessler DM, Jimenez G, Li X, Kolker S, Allen W, Linehan JA, Twardowski PW and Ascierto ML: Impact of intra-tumoral immunity on predicting response and survival after neoadjuvant cisplatin-based chemotherapy in patients with muscle invasive bladder cancer. Cancer Med 13: e70088, 2024.
138. Cai X, Yang J, Guo Y, Yu Y, Zheng C and Dai X: Re-analysis of single cell and spatial transcriptomics data reveals B cell landscape in gastric cancer microenvironment and its potential crosstalk with tumor cells for clinical prognosis. J Transl Med 22: 807, 2024.
139. Liu Z, Yang Y, Fang H, Cen B, Fan Y, Li J, Wang L and He S: Single-cell and spatial analyses reveal the effect of VSIG4(+) S100A10(+)TAMs on the immunosuppression of glioblastoma and anti-PD-1 immunotherapy. Int J Biol Macromol 308: 142415, 2025.
140. Gao W, Long X, Lin X, Deng K, Li D, Huang M, Wang X, Liu Q and Wu M: Targeting mesenchymal monocyte-derived macrophages to enhance the sensitivity of glioblastoma to temozolomide by inhibiting TNF/CELSR2/p65/Kla-HDAC1/EPAS1 axis. J Adv Res 80: 925-941, 2026.
141. Shekarian T, Ritz MF, Hogan S, Martins TA, Schmassmann P, Gerber A, Roux J, Kaymak D, Durano C, Burger B, *et al*: Multidimensional analysis of matched primary and recurrent glioblastoma identifies contributors to tumor recurrence influencing time to relapse. J Neuropathol Exp Neurol 84: 45-58, 2025.
142. Xu H, Chai H, Chen M, Zhu R, Jiang S, Liu X, Wang Y, Chen J, Wei J, Mao Y and Shi Z: Single-cell RNA sequencing identifies a subtype of FN1 + tumor-associated macrophages associated with glioma recurrence and as a biomarker for immunotherapy. Biomark Res 12: 114, 2024.
143. Prawira A, Xu H, Mei Y, Leow WQ, Nasir NJM, Reolo MJ, Otsuka M, Rahbari M, Chen Z, Weerasooriya M, *et al*: Targeting Treg-fibroblast interaction to enhance immunotherapy in steatotic liver disease-related hepatocellular carcinoma. Gut 75: 105-118, 2025.
144. Xu W, Weng J, Zhao Y, Xie P, Xu M, Liu S, Yu Q, Yu M, Liang B, Chen J, *et al*: FMO2(+) cancer-associated fibroblasts sensitize anti-PD-1 therapy in patients with hepatocellular carcinoma. J Immunother Cancer 13: e011648, 2025.
145. Hirose K, Motooka D, Hayashi Y and Hori Y: Elucidating disease pathogenesis using formalin-fixed paraffin-embedded samples: Integrating genomics, spatial transcriptomics, and histology-A focus on vascular anomalies. J Oral Biosci 68: 100779, 2026.
146. Frangieh CJ, Fan JL, Melms JC, Shah P, Azizi E and Izar B: Single-cell and spatial profiling in cancer biology and clinical oncology. Nat Cancer 7: 597-607, 2026.
147. Thanormjit K, Suwatthanarak T, Arigul T, Chaiboonchoe A, Acharayothin O, Jenjaroenpun P, Chinswangwatanakul V and Tanjak P: Comparative spatial whole transcriptome analysis of matched frozen and formalin-fixed paraffin-embedded colorectal cancer tissues. Biochem Biophys Rep 45: 102413, 2026.
148. Yan C, Corbett RD, Trinh D, Jin D, Laskin J, Bailey ML and Marra MA: Single-cell analysis of matched FFPE and frozen tissue samples reveals comparable resolution of intratumoural heterogeneity. Front Genet 17: 1755978, 2026.
149. Wulf MG, Maguire S, Dai N, Blondel A, Posfai D, Krishnan K, Sun Z, Guan S and Correa IR: Chemical capping improves template switching and enhances sequencing of small RNAs. Nucleic Acids Res 50: e2, 2022.
150. Liu X and Ren X: Computational strategies and algorithms for inferring cellular composition of spatial transcriptomics data. Genomics Proteomics Bioinformatics 22: qzae057, 2024.
151. Mo CK, Liu J, Chen S, Storrs E, Targino da Costa ALN, Houston A, Wendl MC, Jayasinghe RG, Iglesia MD, Ma C, *et al*: Tumour evolution and microenvironment interactions in 2D and 3D space. Nature 634: 1178-1186, 2024.
152. Pentimalli TM, Karaiskos N and Rajewsky N: Challenges and opportunities in the clinical translation of High-resolution spatial transcriptomics. Annu Rev Pathol 20: 405-432, 2025.
153. Kukanja P, Langseth CM, Rubio Rodriguez-Kirby LA, Agirre E, Zheng C, Raman A, Yokota C, Avenel C, Tiklova K, Guerreiro-Cacais AO, *et al*: Cellular architecture of evolving neuroinflammatory lesions and multiple sclerosis pathology. Cell 187: 1990-2009.e19, 2024.
154. Heidari E, Moorman A, Unyi D, Pasnuri N, Rukhovich G, Calafato D, Mathioudaki A, Chan JM, Nawy T, Gerstung M, *et al*: Segger: Fast and accurate cell segmentation of imaging-based spatial transcriptomics data. bioRxiv: Mar 16, 2025 doi:10.1101/2025.03.14.643160.
155. Yu H, Carroll AY, Shen K, Wu N, Yan H, Xiong J, Mercado MF, Kaiser EA, Gautam M, Li M, *et al*: Segmentation matters: Recognizing the cell segmentation challenge in spatial transcriptomics. bioRxiv: Aug 29, 2025 doi: 10.1101/2025.08.25.672145.
156. Mitchel J, Gao T, Petukhov V, Cole E and Kharchenko PV: Impact and correction of segmentation errors in spatial transcriptomics. Nat Genet 58: 434-444, 2026.
157. Kamboj O, Park J, Stegle O and Hamprecht FA: From spots to cells: Cell segmentation in spatial transcriptomics with BOMS. PLoS One 20: e0311458, 2025.
158. Littman R, Hemminger Z, Foreman R, Arneson D, Zhang G, Gomez-Pinilla F, Yang X and Wollman R: Joint cell segmentation and cell type annotation for spatial transcriptomics. Mol Syst Biol 17: e10108, 2021.
159. Ma Y and Zhou X: Spatially informed cell-type deconvolution for spatial transcriptomics. Nat Biotechnol 40: 1349-1359, 2022.
160. Zhang J, Qiao X, Zhang L and Guo W: BASIN: Bayesian mAtrix variate normal model with Spatial and sparsIty priors in Non-negative deconvolution. ArXiv: Oct 24, 2025.
161. Gaspard-Boulinc LC, Gortana L, Walter T, Barillot E and Cavalli FMG: Cell-type deconvolution methods for spatial transcriptomics. Nat Rev Genet 26: 828-846, 2025.
162. Li Y and Zhang S: Statistical batch-aware embedded integration, dimension reduction, and alignment for spatial transcriptomics. Bioinformatics 40: btae611, 2024.
163. Pratama R, Hilton J, Cherry JM and Song G: Gene spatial integration: Enhancing spatial transcriptomics analysis via deep learning and batch effect mitigation. Bioinformatics 41: btaf350, 2025.
164. Fang D and Min W: SpaCross deciphers spatial structures and corrects batch effects in multi-slice spatially resolved transcriptomics. Commun Biol 8: 1393, 2025.
165. Cesaro G, Nagai JS, Gnoato N, Chiodi A, Tussardi G, Kloker V, Musumarra CV, Mosca E, Costa IG, Di Camillo B, *et al*: Advances and challenges in cell-cell communication inference: A comprehensive review of tools, resources, and future directions. Brief Bioinform 26: bbaf280, 2025.
166. Dries R, Zhu Q, Dong R, Eng CL, Li H, Liu K, Fu Y, Zhao T, Sarkar A, Bao F, *et al*: Giotto: A toolbox for integrative analysis and visualization of spatial expression data. Genome Biol 22: 78, 2021.
167. Palla G, Spitzer H, Klein M, Fischer D, Schaar AC, Kuemmerle LB, Rybakov S, Ibarra IL, Holmberg O, Virshup I, *et al*: Squidpy: A scalable framework for spatial omics analysis. Nat Methods 19: 171-178, 2022.
168. Qiu X, Zhu DY, Lu Y, Yao J, Jing Z, Min KH, Cheng M, Pan H, Zuo L, King S, *et al*: Spatiotemporal modeling of molecular holograms. Cell 187: 7351-7373.e61, 2024.
169. Liu J, Manabe H, Qian W, Orikasa S, Ghaemmaghami J, Wang Y, Gu Y, Chu AKY, Gadhvi G, Song Y, *et al*: CytoSignal detects locations and dynamics of ligand-receptor signaling at cellular resolution from spatial transcriptomic data. Nat Genet 58: 1396-1408, 2026.
170. Cang Z, Zhao Y, Almet AA, Stabell A, Ramos R, Plikus MV, Atwood SX and Nie Q: Screening cell-cell communication in spatial transcriptomics via collective optimal transport. Nat Methods 20: 218-228, 2023.
171. Li S, Wang R, Liu S and Li SC: Finding spatially variable ligand-receptor interactions with functional support from downstream genes. Nat Commun 16: 7784, 2025.
172. You Y, Fu Y, Li L, Zhang Z, Jia S, Lu S, Ren W, Liu Y, Xu Y, Liu X, *et al*: Systematic comparison of sequencing-based spatial transcriptomic methods. Nat Methods 21: 1743-1754, 2024.
173. Plummer JT, Dezem FS, Cook DP, Park J, Zhang L, Liu Y, Marcao M, DuBose H, Wani A, Wise K, *et al*: Standardized metrics for assessment and reproducibility of imaging-based spatial transcriptomics datasets. Nat Biotechnol 44: 1213-1225, 2026.

174. Song W, Wang D, Li J and Zhang R: Spatial transcriptomics: Integrating platforms and computational approaches for clinical insights. Biotechnol Adv 87: 108791, 2026.
175. Zhu J, Deng R, Guo J, Yao T, Lu S, Qu C, Xiong J, Zhu Y, Lu Z, Yang Y, *et al*: Computer vision methods for spatial transcriptomics: A survey. bioRxiv: Oct 14, 2025 doi: 10.1101/2025.10.13.682148.
176. Tran KA, Kondrashova O, Bradley A, Williams ED, Pearson JV and Waddell N: Deep learning in cancer diagnosis, prognosis and treatment selection. Genome Med 13: 152, 2021.
177. Cruz JA and Wishart DS: Applications of machine learning in cancer prediction and prognosis. Cancer Inform 2: 59-77, 2007.
178. Layton AT: AI, machine learning, and ChatGPT in hypertension. Hypertension 81: 709-716, 2024.
179. Rauschert S, Raubenheimer K, Melton PE and Huang RC: Machine learning and clinical epigenetics: A review of challenges for diagnosis and classification. Clin Epigenetics 12: 51, 2020.
180. Lo Vercio L, Amador K, Bannister JJ, Crites S, Gutierrez A, MacDonald ME, Moore J, Mouches P, Rajashekar D, Schimert S, *et al*: Supervised machine learning tools: A tutorial for clinicians. J Neural Eng: Nov 19, 2020 (Epub ahead of print). doi: 10.1088/1741-2552/abbff2.
181. Tejada-Lapuerta A, Schaar AC, Gutgesell R, Palla G, Halle L, Minaeva M, Vornholz L, Dony L, Drummer F, Richter T, *et al*: Nicheformer: A foundation model for single-cell and spatial omics. Nat Methods 22: 2525-2538, 2025.
182. Blampey Q, Benkirane H, Bercovici N, Mulder K, Gessain G, Ginhoux F, Andre F and Cournede PH: Novae: A graph-based foundation model for spatial transcriptomics data. Nat Methods 22: 2539-2550, 2025.
183. Ji T, Yang B, Wang M, Ji H, Yang H and Liu Y: AugGCL: Multimodal graph learning for spatial transcriptomics analysis with enhanced gene and morphological data. PLoS Comput Biol 22: e1013912, 2026.
184. Wang C and Yu X: STransfer: A transfer learning-enhanced graph convolutional network for clustering spatial transcriptomics data. Bioinformatics 42: btag049, 2026.
185. Liu T, Huang T, Jin W, Chu T, Ying R and Zhao H: spRefine denoises and imputes spatial transcriptomics with a Reference-free framework powered by genomic language model. bioRxiv: Jul 7, 2025 (Epub ahead of print). doi: 10.1101/2025.04.22.649977.
186. Xu Y, Yu B, Chen X, Peng A, Tao Q, He Y, Wang Y and Li XM: DSCT: A novel deep-learning framework for rapid and accurate spatial transcriptomic cell typing. Natl Sci Rev 12: nwaf030, 2025.
187. Peng H, Wu X, Liu S, He M, Tang C, Wen Y, Xie C, Zhong R, Li C, Xiong S, *et al*: Cellular dynamics in tumour microenvironment along with lung cancer progression underscore spatial and evolutionary heterogeneity of neutrophil. Clin Transl Med 13: e1340, 2023.
188. Roller A, Davydov, II, Schwalie PC, Serrano-Serrano ML, Heller A, Staedler N, Ferreira CS, Dietmann G, Klaman I and Valdeolivas A: Tumor-agnostic transcriptome-based classifier identifies spatial infiltration patterns of CD8+T cells in the tumor microenvironment and predicts clinical outcome in early-phase and late-phase clinical trials. J Immunother Cancer 12: e008185, 2024.
189. Sun H, Han X, Du Z, Chen G, Guo T, Xie F, Gu W and Shi Z: Machine learning for the identification of neoantigen-reactive CD8 + T cells in gastrointestinal cancer using single-cell sequencing. Br J Cancer 131: 387-402, 2024.
190. Chen C, Wang J, Pan D, Wang X, Xu Y, Yan J, Wang L, Yang X, Yang M and Liu GP: Applications of multi-omics analysis in human diseases. MedComm (2020) 4: e315, 2023.
191. Jin Y, Wu Y, Reuben A, Zhu L, Gay CM, Wu Q, Zhou X, Mo H, Zheng Q, Ren J, *et al*: Single-cell and spatial proteo-transcriptomic profiling reveals immune infiltration heterogeneity associated with neuroendocrine features in small cell lung cancer. Cell Discov 10: 93, 2024.
192. Aung TN, Monkman J, Warrell J, Vathiotis I, Bates KM, Gavrielatou N, Trontzas IP, Tan CW, Fernandez AI, Moutafi M, *et al*: Spatial signatures for predicting immunotherapy outcomes using multi-omics in non-small cell lung cancer. Nat Genet 57: 2482-2493, 2025.
193. O'Connell BC, Hubbard C, Zizlsperger N, Fitzgerald D, Kutok JL, Varner J, Ilaria R Jr, Cobleigh MA, Juric D, Tkaczuk KHR, *et al*: Eganelisib combined with immune checkpoint inhibitor therapy and chemotherapy in frontline metastatic triple-negative breast cancer triggers macrophage reprogramming, immune activation and extracellular matrix reorganization in the tumor microenvironment. J Immunother Cancer 12: e009160, 2024.
194. Wu Z, Boen J, Jindal S, Basu S, Bieniosek M, He S, LaPelusa M, Mayer AT, Kaseb AO, Zou J, *et al*: Spatial multi-omics and deep learning reveal fingerprints of immunotherapy response and resistance in hepatocellular carcinoma. bioRxiv: Jun 12, 2025 (Epub ahead of print). doi: 10.1101/2025.06.11.656869.
195. Stupichev D, Miheecheva N, Postovalova E, Lyu Y, Ramachandran A, Galkin I, Khegai G, Perevoshchikova K, Love A, Menshikova S, *et al*: AI-driven multimodal algorithm predicts immunotherapy and targeted therapy outcomes in clear cell renal cell carcinoma. Cell Rep Med 6: 102299, 2025.
196. He B, Bergenstrahle L, Stenbeck L, Abid A, Andersson A, Borg A, Maaskola J, Lundeberg J and Zou J: Integrating spatial gene expression and breast tumour morphology via deep learning. Nat Biomed Eng 4: 827-834, 2020.
197. Bell ATF, Mitchell JT, Kiemen AL, Lyman M, Fujikura K, Lee JW, Coyne E, Shin SM, Nagaraj S, Deshpande A, *et al*: PanIN and CAF transitions in pancreatic carcinogenesis revealed with spatial data integration. Cell Syst 15: 753-769.e5, 2024.